

Interplay between Pair Density Wave and a Nested Fermi Surface

Jin-Tao Jin,¹ Kun Jiang,^{2,3,*} Hong Yao,^{4,5,†} and Yi Zhou^{2,3,1,6,‡}

¹Kavli Institute for Theoretical Sciences, University of Chinese Academy of Sciences, Beijing 100190, China

²Institute of Physics, Chinese Academy of Sciences, Beijing 100190, China

³Songshan Lake Materials Laboratory, Dongguan, Guangdong 523808, China

⁴Institute for Advanced Study, Tsinghua University, Beijing 100084, China

⁵State Key Laboratory of Low Dimensional Quantum Physics, Tsinghua University, Beijing 100084, China

⁶CAS Center for Excellence in Topological Quantum Computation,
University of Chinese Academy of Sciences, Beijing 100190, China

(Dated: April 12, 2022)

We show that spontaneous time-reversal-symmetry (TRS) breaking can naturally arise from the interplay between pair density wave (PDW) ordering at multiple momenta and nesting of Fermi surfaces (FS). Concretely, we consider pair-density-wave superconductivity on a hexagonal lattice with nested FS at $3/4$ electron filling, which is related to a recently discovered superconductor CsV_3Sb_5 . Because of nesting of the FS, each momentum \mathbf{k} on the FS has at least two counterparts $-\mathbf{k} \pm \mathbf{Q}_\alpha$ ($\alpha = 1, 2, 3$) on the FS to form finite momentum ($\pm \mathbf{Q}_\alpha$) Cooper pairs, resulting in a TRS and inversion broken PDW state with stable Bogoliubov Fermi pockets. Various spectra, including (local) density of states, electron spectral function and the effect of quasi-particle interference, have been investigated. The partial melting of the PDW will give rise to 4×4 and $\frac{4}{\sqrt{3}} \times \frac{4}{\sqrt{3}}$ CDW orders, in addition to the 2×2 CDW. Possible implications to real materials such as CsV_3Sb_5 and future experiments have been further discussed.

Introduction. — A pair density wave (PDW) is a superconducting (SC) state in which Cooper pairs carry finite momentum and its SC order parameter is spatially modulated without applying external magnetic field [1–19] (for a recent review, see, e.g. Ref. [20]). Such kind of state is similar to the one proposed earlier by Fulde-Ferrell (FF) [21] and Larkin-Ovchinnikov (LO) [22] (together known as FFLO) in magnetic field above the Pauli limit. As a mother state for various descendant orders, e.g., charge density wave (CDW), loop current, and charge- $4e$ superconductivity, PDW has been receiving increasing attentions from diverse fields in physics, ranging from condensed matter [20] to high energy physics [23]. In particular, PDW was recently proposed as a promising candidate for explaining various interesting phenomena in cuprates and other strongly correlated systems [20, 24–27].

In previous studies of PDW in systems with generic FS, only electrons near hot spots on FS can come into being finite momentum Cooper pairs and are gapped, while other parts of FS remain gapless. In contrast, as will be revealed in this work, the FS nesting feature admits full PDW pairing around the FS, that will gain more condensation energy than the partial pairing usually, while in-gap quasi-particle excitations are still allowed. Thus, it would be of great interest to examine the interplay between these two, PDW and FS nesting. (Note that the role of FS nesting was considered mostly to the ordering of CDW or spin-density-wave in general, e.g. see Ref. [28–33]).

In this letter, we study PDW ordering in the presence of a nested FS of electrons in a system with hexagonal symmetry such as Kagome lattice and triangular lattice. We found that a time reversal symmetry (TRS) breaking PDW state is favored with lower condensation energy. Bogoliubov quasi-particle excitations, density of states (DOS), local density of states (LDOS), and electron spectral function will be investigated as well as the quasi-particle interference (QPI) in scanning

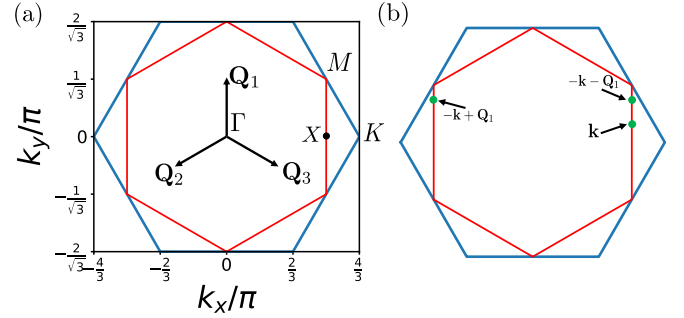


FIG. 1. First Brillouin zone (BZ) of a hexagonal lattice and nesting feature of PDW. (a) BZ and the nested FS at $3/4$ filling. The boundary of BZ is in blue and red lines represent the FS. (b) Each \mathbf{k} on a FS segment along the \mathbf{Q}_α direction has two counterparts $-\mathbf{k} \pm \mathbf{Q}_\alpha$ on the FS to form finite momentum ($\pm \mathbf{Q}_\alpha$) Cooper pairs.

tunnelling microscopy (STM) experiments. The implications to recently discovered Kagome SC AV_3Sb_5 ($A = \text{K, Rb, Cs}$) will also be discussed.

Model. — We start with a single band model on a hexagonal lattice, on which the FS is nested as illustrated in Fig. 1. In the presence of finite momentum Cooper pairing, the Hamiltonian takes the form,

$$H = \sum_{\mathbf{k}, \sigma} \xi_{\mathbf{k}} c_{\mathbf{k}, \sigma}^\dagger c_{\mathbf{k}, \sigma} + \sum_{\mathbf{k}, \alpha} \left[\Delta_{\mathbf{Q}_\alpha}(\mathbf{k}) c_{\mathbf{k}, \uparrow}^\dagger c_{-\mathbf{k} + \mathbf{Q}_\alpha, \downarrow}^\dagger + \Delta_{-\mathbf{Q}_\alpha}(\mathbf{k}) c_{\mathbf{k}, \uparrow}^\dagger c_{-\mathbf{k} - \mathbf{Q}_\alpha, \downarrow}^\dagger + h.c. \right], \quad (1)$$

where $c_{\mathbf{k}, \sigma}^\dagger$ ($c_{\mathbf{k}, \sigma}$) is electron creation (annihilation) operator with momentum \mathbf{k} and spin $\sigma = \uparrow, \downarrow$, $\xi_{\mathbf{k}} = \epsilon_{\mathbf{k}} - \mu$ is the energy measured from the chemical potential μ . $\Delta_{\pm \mathbf{Q}_\alpha}(\mathbf{k}) = \Delta_{\pm \mathbf{Q}_\alpha} \exp[-(|\xi_{\mathbf{k}}| + |\xi_{-\mathbf{k} \pm \mathbf{Q}_\alpha}|)/(2\Lambda)]$ ($\alpha = 1, 2, 3$) indicates the Cooper pairing of two electrons with total momentum $\pm \mathbf{Q}_\alpha$. Here a smooth energy cutoff Λ is introduced, the lattice

constant is set to be $a = 1$. We consider the following \mathbf{Q}_α : $\mathbf{Q}_1, \mathbf{Q}_2, \mathbf{Q}_3 = \left(0, \frac{\pi}{\sqrt{3}}\right), \left(-\frac{\pi}{2}, -\frac{\pi}{2\sqrt{3}}\right), \left(\frac{\pi}{2}, -\frac{\pi}{2\sqrt{3}}\right)$ since they are most relevant to CsV_3Sb_5 for which experimental evidences of period 4 PDW was recently reported [34]. As shown in Fig. 1(a), the first Brillouin zone (BZ) is a hexagon, and we consider a hexagonal and nested FS, which can be realized by choosing the chemical potential μ or the electron filling properly. As a simple example, we focus on a triangular lattice, set the nearest neighboring (NN) hopping integral $t = 1$, and choose chemical potential $\mu = 2$ (or $3/4$ electron filling), such that $\xi_{\mathbf{k}} = -2 \left[\cos(k_x) + \cos\left(\frac{1}{2}k_x + \frac{\sqrt{3}}{2}k_y\right) + \cos\left(\frac{1}{2}k_x - \frac{\sqrt{3}}{2}k_y\right) + 1 \right]$. Note that main results obtained in this work will also be applicable to more generic situations, including honeycomb and kagome lattices.

From Fig. 1(b), one sees that each \mathbf{k} on a FS segment along the \mathbf{Q}_α direction has at least two counterparts $-\mathbf{k} \pm \mathbf{Q}_\alpha$ to form finite momentum Cooper pairs on the FS. Moreover, M and X points have four momenta for pairing. These mean that the nesting feature allows *full pairing* in the region near the FS, which is in contrast with generic FS without nesting.

Time reversal symmetry. — The TRS of the Hamiltonian is respected if and only if $\xi_{-\mathbf{k}} = \xi_{\mathbf{k}}$ and $\Delta_{\mathbf{Q}_\alpha}^*(\mathbf{k} + \mathbf{Q}_\alpha) = \Delta_{-\mathbf{Q}_\alpha}(\mathbf{k})$ for any \mathbf{k} . For the aforementioned form of $\Delta_{\pm\mathbf{Q}_\alpha}(\mathbf{k})$, sufficient and necessary conditions for TRS reduce to $\Delta_{\mathbf{Q}_\alpha}^* = \Delta_{-\mathbf{Q}_\alpha}$.

The finite momentum pairing $\Delta_{\pm\mathbf{Q}_\alpha}(\mathbf{k})$ leads to a spatially varying pairing function $\Delta(\mathbf{r})$ in real space, resulting in a PDW. To be simple, we set $\Delta_{\pm\mathbf{Q}_\alpha} = \Delta e^{i\theta_\alpha} e^{\pm i\frac{\theta_\alpha}{2}}$ for all α , where Δ is real and positive, $\theta_\alpha \in (-\pi, \pi]$ is the overall phase of $\Delta_{\pm\mathbf{Q}_\alpha}$ and $\phi_\alpha \in (-\pi, \pi]$ is the phase difference between $\Delta_{\mathbf{Q}_\alpha}$ and $\Delta_{-\mathbf{Q}_\alpha}$. Thus the pairing function $\Delta(\mathbf{r})$ reads

$$\Delta(\mathbf{r}) = 2\Delta \sum_{\alpha} e^{i\theta_\alpha} \cos\left(\mathbf{Q}_\alpha \cdot \mathbf{r} + \frac{\phi_\alpha}{2}\right). \quad (2)$$

Commensurate PDW and descendant CDW order. — When the PDW melts in part, i.e., the $U(1)$ gauge symmetry is restored but not the translational symmetry, a descendant CDW order will arise with wave vectors $\mathbf{q} = \pm\mathbf{Q}_\alpha \pm \mathbf{Q}_\beta \neq \mathbf{0}$. These CDW wave vectors can be classified into three sets B, C and D as follows: (B) $\mathbf{q} = \pm\mathbf{Q}_\alpha$ associated with a 4×4 CDW; (C) $\mathbf{q} = \pm 2\mathbf{Q}_\alpha$ associated with a 2×2 CDW; (D) $\mathbf{q} = \pm(\mathbf{Q}_\alpha - \mathbf{Q}_\beta)$ associated with a $\frac{4}{\sqrt{3}} \times \frac{4}{\sqrt{3}}$ CDW [see Fig. 3(c)]. Note that the FS is nested by wave vectors $\mathbf{q} = \pm 2\mathbf{Q}_\alpha$ in C but not those in B or D. So that the descendant CDW order can be of 4×4 and $\frac{4}{\sqrt{3}} \times \frac{4}{\sqrt{3}}$, in addition to the 2×2 CDW that also originates from the FS nesting.

Bogoliubov quasi-particles. — To study quasi-particle excitations in such a commensurate PDW associated with a 4×4 folding of the BZ, we introduce a row of creation operators,

$$\begin{aligned} \hat{c}_{\mathbf{k},\sigma}^\dagger = & \left(\hat{c}_{\mathbf{k},\sigma}^\dagger, \hat{c}_{\mathbf{k}+\mathbf{Q}_1,\sigma}^\dagger, \hat{c}_{\mathbf{k}-\mathbf{Q}_1,\sigma}^\dagger, \hat{c}_{\mathbf{k}+\mathbf{Q}_2,\sigma}^\dagger, \hat{c}_{\mathbf{k}-\mathbf{Q}_2,\sigma}^\dagger, \hat{c}_{\mathbf{k}+\mathbf{Q}_3,\sigma}^\dagger, \hat{c}_{\mathbf{k}-\mathbf{Q}_3,\sigma}^\dagger, \right. \\ & \hat{c}_{\mathbf{k}+2\mathbf{Q}_1,\sigma}^\dagger, \hat{c}_{\mathbf{k}+2\mathbf{Q}_2,\sigma}^\dagger, \hat{c}_{\mathbf{k}+2\mathbf{Q}_3,\sigma}^\dagger, \hat{c}_{\mathbf{k}+\mathbf{Q}_1-\mathbf{Q}_2,\sigma}^\dagger, \hat{c}_{\mathbf{k}-\mathbf{Q}_1+\mathbf{Q}_2,\sigma}^\dagger, \\ & \left. \hat{c}_{\mathbf{k}+\mathbf{Q}_2-\mathbf{Q}_3,\sigma}^\dagger, \hat{c}_{\mathbf{k}-\mathbf{Q}_2+\mathbf{Q}_3,\sigma}^\dagger, \hat{c}_{\mathbf{k}+\mathbf{Q}_3-\mathbf{Q}_1,\sigma}^\dagger, \hat{c}_{\mathbf{k}-\mathbf{Q}_3+\mathbf{Q}_1,\sigma}^\dagger \right), \end{aligned}$$

and rewrite Eq. (1) in a matrix form as follows,

$$\begin{aligned} H &= \frac{1}{16} \sum_{\mathbf{k}} H_{\mathbf{k}} + \sum_{\mathbf{k}} \xi_{\mathbf{k}} \\ &= \frac{1}{16} \sum_{\mathbf{k}} (\hat{c}_{\mathbf{k},\uparrow}^\dagger, \hat{c}_{-\mathbf{k},\downarrow}) \hat{\mathcal{H}}_{\mathbf{k}} \begin{pmatrix} \hat{c}_{\mathbf{k},\uparrow} \\ \hat{c}_{-\mathbf{k},\downarrow}^\dagger \end{pmatrix} + \sum_{\mathbf{k}} \xi_{\mathbf{k}}, \end{aligned} \quad (3a)$$

$$\hat{\mathcal{H}}_{\mathbf{k}} = \begin{pmatrix} \hat{D}(\mathbf{k}) & \hat{\Delta}(\mathbf{k}) \\ \hat{\Delta}^\dagger(\mathbf{k}) & -\hat{D}(-\mathbf{k}) \end{pmatrix}. \quad (3b)$$

Here $\hat{\mathcal{H}}_{\mathbf{k}}$ is a 32×32 matrix, $\hat{D}(\mathbf{k}) = \text{diag}\{\xi_{\mathbf{k}_i}\}$ is a diagonal matrix, \mathbf{k}_i is the i -th momentum in $\hat{c}_{\mathbf{k},\uparrow}^\dagger$, and $\hat{\Delta}(\mathbf{k})$ is a 16×16 pairing matrix defined by $\Delta_{\pm\mathbf{Q}_\alpha}(\mathbf{k})$.

The diagonalization of $\hat{\mathcal{H}}_{\mathbf{k}}$ leads to the quasi-particle energy dispersion as follows,

$$H_{\mathbf{k}} = \sum_{i=1}^{16} E(\mathbf{k})_i^+ \gamma_{\mathbf{k},\uparrow,i}^\dagger \gamma_{\mathbf{k},\uparrow,i} + E(\mathbf{k})_i^- (-\gamma_{-\mathbf{k},\downarrow,i}^\dagger \gamma_{-\mathbf{k},\downarrow,i} + 1), \quad (4)$$

where $E(\mathbf{k})_i^- (i = 16, \dots, 1)$ and $E(\mathbf{k})_i^+ (i = 1, \dots, 16)$ are energy dispersion for quasi-holes and quasi-particles respectively, that are arranged in ascending order. Note that the particle-hole symmetry (PHS) is manifested by $E(\mathbf{k})_i^+ = -E(-\mathbf{k})_i^-$, which would give rise to $E(\mathbf{k})_i^+ = -E(\mathbf{k})_i^-$ if the TRS was respected. $\gamma_{\mathbf{k},\uparrow(\downarrow),i}$'s are Bogoliubov quasi-particle annihilation operators, and the electron operator $\hat{c}_{\mathbf{k},\uparrow,i}^\dagger$ can be written in terms of them,

$$\hat{c}_{\mathbf{k},\uparrow,i}^\dagger = \sum_{j=1}^{16} \left(u(\mathbf{k})_{ij} \gamma_{\mathbf{k},\uparrow,j}^\dagger + v(\mathbf{k})_{ij} \gamma_{-\mathbf{k},\downarrow,j} \right), \quad (5)$$

where $u(\mathbf{k})_{ij}$ and $v(\mathbf{k})_{ij}$ form a unitary transformation. It is easy to verify the following relations: $E(\mathbf{k})_i^s = E(\mathbf{k} \pm \mathbf{Q}_\alpha)_i^s$ and $\gamma_{\mathbf{k},\sigma,i} = \gamma_{\mathbf{k} \pm \mathbf{Q}_\alpha, \sigma, i}$, i.e., the BZ is of 4×4 folding.

\mathbb{Z}_2 symmetry. — It is found that there exists additional \mathbb{Z}_2 symmetries associated with a theorem as follows.

Theorem: For each α , the transformation $\Delta_{\pm\mathbf{Q}_\alpha} \mapsto -\Delta_{\pm\mathbf{Q}_\alpha}$ does not change the energy spectra of the system.

The proof of the theorem can be found in the Supplementary Material [35]. Note that this theorem suggests a $\mathbb{Z}_2 \times \mathbb{Z}_2$ symmetry, since only two of \mathbf{Q}_α are independent.

Approximate $E(\mathbf{k})_1^+$. — To get insight into low energy excitations, we firstly inspect the lowest branch of their energy dispersion, $E(\mathbf{k})_1^+$, along the FS. Without loss of generality, we consider the FS segment $M - X$ [see Figs. 1(a) and 1(b)]. For each \mathbf{k} on this segment and away from M and X points, in consideration of the energy cutoff in $\Delta_{\pm\mathbf{Q}_\alpha}(\mathbf{k})$, it is found that only the pairings between \mathbf{k} and $-\mathbf{k} \pm \mathbf{Q}_1$ are of order of Δ , while other pairing terms are much smaller than them. Keeping these sizable pairing terms in $\hat{\Delta}(\mathbf{k})$ and neglecting others, we find that $\hat{\mathcal{H}}_{\mathbf{k}}$ can be approximately decomposed into the direct sum of paired and unpaired parts, i.e., $\hat{\mathcal{H}}_{\mathbf{k}} \approx \hat{\mathcal{H}}_{\mathbf{k}}^p \oplus \hat{\mathcal{H}}_{\mathbf{k}}^f$ [35]. Therefore $E(\mathbf{k})_1^+$ can be estimated as follows,

$$E(\mathbf{k})_1^+ \approx \min\{E^p(\mathbf{k}), E^f(\mathbf{k})\}, \quad (6a)$$

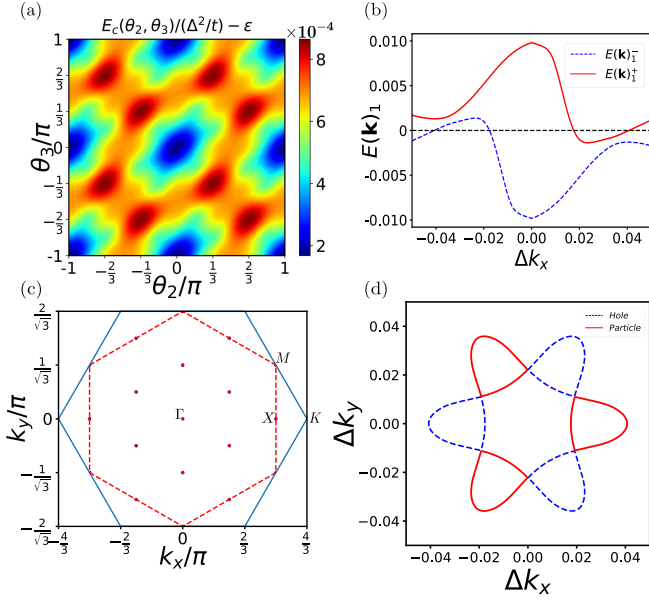


FIG. 2. (a) Condensation energy E_c as a function of θ_2 and θ_3 , where $\theta_1 = 0$ and $\phi_\alpha = \pi/2$ have been set [see Eq. (2)]. A constant energy shift $\varepsilon = 0.993$ is introduced. Maximal E_c occurs at $\theta_2 = \theta_3 - \theta_2 \equiv \pm 2\pi/3 \pmod{\pi}$. (b)-(d) Energy dispersion and Bogoliubov Fermi pockets for the lowest energy state: $\phi_\alpha = \pi/2$, $\theta_1 = 0$, $\theta_2 = 2\pi/3$ and $\theta_3 = -2\pi/3$. (b) Quasi-particle dispersion $E(\mathbf{k})_1^+$ and quasi-hole dispersion $E(\mathbf{k})_1^-$ around the X point that are plotted along the line of $\Gamma - X - K$. (c) The Bogoliubov Fermi pockets at M and X points and their periodic replica due to the PDW. (d) Quasi-particle and quasi-hole pockets around the X point.

where $E^p(\mathbf{k})$ and $E^f(\mathbf{k})$ are lowest non-negative eigenvalues of $\hat{\mathcal{H}}_{\mathbf{k}}^p$ and $\hat{\mathcal{H}}_{\mathbf{k}}^f$ respectively. Straightforward algebra [35] leads to

$$E^p(\mathbf{k}) = 2\Delta \min \left\{ \left| \sin \left(\frac{\phi_1}{2} \right) \right|, \left| \cos \left(\frac{\phi_1}{2} \right) \right| \right\}. \quad (6b)$$

It takes the minimum $E^p(\mathbf{k})_{\min} = 0$ at $\phi_1 = 0, \pi$ and the maximum $E^p(\mathbf{k})_{\max} = \sqrt{2}\Delta$ at $\phi_1 = \pm \pi/2$. Thus, we expect that the condensation of Cooper pairs will gain most energy at $\phi_\alpha = \pm \pi/2$. This can be verified by the numerical diagonalization of $\hat{\mathcal{H}}_{\mathbf{k}}$ as will be discussed. On the other hand, $E^f(\mathbf{k})$ is determined by the diagonal matrix $\hat{\mathcal{H}}_{\mathbf{k}}^f$, and is responsible for (nearly) unpaired electrons and in-gap excitations in $E(\mathbf{k})_1^+$ as long as $E^f(\mathbf{k}) < E^p(\mathbf{k})$. The combination of $E^p(\mathbf{k})$ and $E^f(\mathbf{k})$ gives rise to the approximate $E(\mathbf{k})_1^+$ along the FS segment.

Away from the FS or near M or X point, other pairing terms become considerable and the simple decomposition of $\hat{\mathcal{H}}_{\mathbf{k}}$ does not work any more. To explore the whole BZ, we shall diagonalize $\hat{\mathcal{H}}_{\mathbf{k}}$ numerically, and study the ground state as well as low energy excitations. For this purpose, we set $\Lambda = 0.1$ and $\Delta = 0.02$ hereafter, unless otherwise specified.

Condensation energy. — The condensation energy $E_c \equiv E_n - E_s$, that defined by the energy difference between a SC ground state and corresponding normal state [36], has been found as $E_c = \frac{1}{N} \sum_{\mathbf{k}} \left(\frac{1}{16} \sum_{i=1}^{16} \sum_{s=\pm} \sum_{E(\mathbf{k})_i^s > 0} E(\mathbf{k})_i^s - |\xi_{\mathbf{k}}| \right)$. The

numerical calculation finds that $E_c[\theta_1, \theta_2, \theta_3, \phi_\alpha]$ reaches local maxima at $\phi_\alpha = \pm \pi/2$. This is in good agreement with the above analysis of approximate $E(\mathbf{k})_1^+$ [see Eq. (6)]. Moreover, as shown in Fig. 2 (a), the PDW state acquires maximum E_c at $\phi_\alpha = \pm \pi/2$ and $\theta_2 - \theta_1 = \theta_3 - \theta_2 \equiv \pm 2\pi/3 \pmod{\pi}$, breaking the TRS spontaneously. Owing to the \mathbb{Z}_2 symmetry theorem, ($\theta_\alpha \mapsto \theta_\alpha \pm \pi$), the period is π instead of 2π here.

Ginzburg-Landau free energy. — The TRS breaking and the \mathbb{Z}_2 symmetry theorem can be verified in Ginzburg-Landau (GL) theory. Up to quartic order in $\Delta_{\mathbf{Q}_\alpha}$, the GL free energy can be written as follows[35],

$$\mathcal{F}[\Delta_{\mathbf{Q}_\alpha}] = \mathcal{F}^{(0)} + \mathcal{F}^{(2)}[\Delta_{\mathbf{Q}_\alpha}] + \mathcal{F}^{(4)}[\Delta_{\mathbf{Q}_\alpha}], \quad (7)$$

where the zero-th order $\mathcal{F}^{(0)}$ is independent of $\Delta_{\mathbf{Q}_\alpha}$, the quadratic term $\mathcal{F}^{(2)} = g^{(2)} \sum_{\alpha=1}^3 \left(|\Delta_{\mathbf{Q}_\alpha}|^2 + |\Delta_{-\mathbf{Q}_\alpha}|^2 \right)$ gives rise to non-vanishing $\Delta_{\mathbf{Q}_\alpha}$ as long as $g^{(2)} < 0$, and the quartic term $\mathcal{F}^{(4)}$ can be further written as $\mathcal{F}^{(4)} = \mathcal{F}_0^{(4)} + \mathcal{F}_\phi^{(4)} + \mathcal{F}_\theta^{(4)}$. Here $\mathcal{F}_0^{(4)}$ depends on the amplitude of the order parameter, $|\Delta_{\mathbf{Q}_\alpha}|$, only. $\mathcal{F}_\phi^{(4)}$ and $\mathcal{F}_\theta^{(4)}$ are given by

$$\mathcal{F}_\phi^{(4)} = g_\phi^{(4)} \left[\left(\Delta_{\mathbf{Q}_1}^2 \right) \left(\Delta_{-\mathbf{Q}_1}^2 \right)^* + \left(\Delta_{\mathbf{Q}_2}^2 \right) \left(\Delta_{-\mathbf{Q}_2}^2 \right)^* + \left(\Delta_{\mathbf{Q}_3}^2 \right) \left(\Delta_{-\mathbf{Q}_3}^2 \right)^* + c.c. \right] \quad (8a)$$

and

$$\mathcal{F}_\theta^{(4)} = g_\theta^{(4)} \left[(\Delta_{\mathbf{Q}_1} \Delta_{-\mathbf{Q}_1}) (\Delta_{\mathbf{Q}_2} \Delta_{-\mathbf{Q}_2})^* + (\Delta_{\mathbf{Q}_2} \Delta_{-\mathbf{Q}_2}) (\Delta_{\mathbf{Q}_3} \Delta_{-\mathbf{Q}_3})^* + (\Delta_{\mathbf{Q}_3} \Delta_{-\mathbf{Q}_3}) (\Delta_{\mathbf{Q}_1} \Delta_{-\mathbf{Q}_1})^* + c.c. \right], \quad (8b)$$

respectively, where both $g_\phi^{(4)}$ and $g_\theta^{(4)}$ are found to be positive and $\Delta_{\mathbf{Q}_\alpha}$ -independent [35]. Putting the PDW ansatz $\Delta_{\pm \mathbf{Q}_\alpha} = \Delta e^{i\theta_\alpha} e^{\pm i\frac{\phi_\alpha}{2}}$ into the above, we obtain $\mathcal{F}_\phi^{(4)} = 2g_\phi^{(4)} \Delta^4 \sum_{\alpha=1}^3 \cos(2\phi_\alpha)$ and $\mathcal{F}_\theta^{(4)} = 2g_\theta^{(4)} \Delta^4 [\cos(2\theta_2 - 2\theta_1) + \cos(2\theta_3 - 2\theta_2) + \cos(2\theta_1 - 2\theta_3)]$. Thus, the lowest free energy is achieved at $\phi_\alpha = \pm \pi/2$ and $\theta_2 - \theta_1 = \theta_3 - \theta_2 \equiv \pm 2\pi/3 \pmod{\pi}$.

Henceforward, we shall focus on the lowest energy state with $\theta_1 = 0$, $\theta_2 = 2\pi/3$, $\theta_3 = -2\pi/3$ and $\phi_\alpha = \pi/2$, and study electronic spectra measured by various experiments.

Bogoliubov Fermi pockets. — As shown in Fig. 2 (b), around M and X points, quasi-particle branch $E(\mathbf{k})_1^+$ sinks down while quasi-hole branch $E(\mathbf{k})_1^-$ rises up, such that both of them go across zero energy. This means that Bogoliubov quasi-particles and quasi-holes possess Fermi surface indeed. In another word, Bogoliubov quasi-particle and quasi-hole pockets come into being. These Fermi pockets are located at M and X points and their periodic replica by the PDW (shifted by a wave vector of the descendant CDW order, $\mathbf{q} = \pm \mathbf{Q}_\alpha \pm \mathbf{Q}_\beta \neq \mathbf{0}$), as indicated in Fig. 2 (c). It is displayed in Fig. 2 (d) that these Fermi pockets exhibit D_3 symmetry.

Density of States. — The differential conductance dI/dV measured by STM [37] is proportional to the DOS that is given by $\rho(\omega) = -\frac{1}{8N} \sum_{\mathbf{k}} \sum_{i,j=1}^{16} \left[|u(\mathbf{k})_{ij}|^2 \frac{\partial n_F(\omega - E(\mathbf{k})_i^+)}{\partial \omega} + |v(\mathbf{k})_{ij}|^2 \frac{\partial n_F(\omega - E(\mathbf{k})_j^-)}{\partial \omega} \right]$, where $n_F(E) = [\exp(E/(k_B T)) + 1]^{-1}$ is

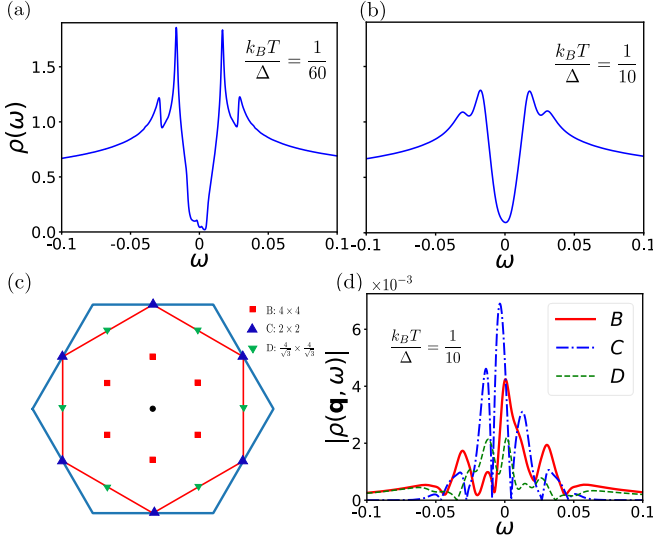


FIG. 3. DOS and LDOS. DOS $\rho(\omega)$ at (a) $k_B T / \Delta = 1/60$ and (b) $k_B T / \Delta = 1/10$. (c) Wave vectors $\mathbf{q} = \pm \mathbf{Q}_\alpha \pm \mathbf{Q}_\beta$ (or their equivalent vectors in first BZ) associated with descendant CDW orders (B: $\mathbf{q} = \pm \mathbf{Q}_\alpha$ or 4×4 , C: $\mathbf{q} = \pm 2\mathbf{Q}_\alpha$ or 2×2 , D: $\mathbf{q} = \pm (\mathbf{Q}_\alpha - \mathbf{Q}_\beta)$ or $4/\sqrt{3} \times 4/\sqrt{3}$). (d) LDOS $\rho(\mathbf{q}, \omega)$ exhibits three types of CDW orders B, C and D. Here $\Lambda = 0.1$ and $\Delta = 0.02$ have been chosen.

the Fermi-Dirac distribution function. The coefficients $u(\mathbf{k})_{ij}$ and $v(\mathbf{k})_{ij}$ are found in accordance with Eqs. (5). As demonstrated in Fig. 3, for $k_B T = \Delta/60 \ll \Delta$, $\rho(\omega)$ exhibits a mini-gap inside the SC gap manifested by sharp coherence peaks; while for $k_B T = \Delta/10 \lesssim \Delta$, $\rho(\omega)$ (thereby dI/dV) curve is of V-shape. Note that both the mini-gap and the V-shape DOS suggest electronic excitations inside the SC gap. It is also worth noting that extra peaks outside sharp coherence peaks are attributed to the Van Hove singularity [38], and the asymmetry between $\rho(\omega)$ and $\rho(-\omega)$ is due to the broken particle-hole symmetry in $\xi_{\mathbf{k}}$.

Local density of states. — Now we go further to study the LDOS or its Fourier transformation $\rho(\mathbf{q}, \omega)$ that serves as a standard tool to identify CDW orders by STM. It is natural to probe a PDW through its descendant CDW orders with the help of LDOS. The LDOS for the PDW state is given by $\rho(\mathbf{q}, \omega) = -\frac{1}{8N} \sum_{\mathbf{k}} \sum_{i,j=1}^{16} \left[u(\mathbf{k})_{ij} u^*(\mathbf{k} + \mathbf{q})_{ij} \frac{\partial n_F(\omega - E(\mathbf{k})_j^+)}{\partial \omega} + v(\mathbf{k})_{ij} v^*(\mathbf{k} + \mathbf{q})_{ij} \frac{\partial n_F(\omega - E(\mathbf{k})_j^-)}{\partial \omega} \right] \bar{\delta}_{\mathbf{k}, \mathbf{k} + \mathbf{q}}$, where $\bar{\delta}$ is the Kronecker comb defined by $\bar{\delta}_{\mathbf{k}, \mathbf{k}'} \equiv \sum_{n,m=-\infty}^{\infty} \delta_{\mathbf{k} + n\mathbf{Q}_1 + m\mathbf{Q}_2, \mathbf{k}'}$ [35]. It has been found that $\rho(\mathbf{q}, \omega)$ does not vanish only at finite number of \mathbf{q} -points in BZ, as labelled in Fig. 3(c). These \mathbf{q} -points are nothing but aforementioned wave vectors of the descendant CDW order. It is noted that $|\rho(\mathbf{q}, \omega)|$ takes the same value at \mathbf{q} -points within each set of B, C or D [35]. As demonstrated in Fig. 3(d), $|\rho(\mathbf{q}, \omega)|$ displays both (B) 4×4 and (D) $4/\sqrt{3} \times 4/\sqrt{3}$ CDW orders in addition to (C) 2×2 CDW order caused by the FS nesting. Define the integrated intensity of these CDW orders as $I_{CDW}(\mathbf{q}) = |\int \rho(\mathbf{q}, \omega) d\omega| / |\int \rho(\mathbf{q} = \mathbf{0}, \omega) d\omega|$, we find that $I_{CDW}^B = 1.51 \times 10^{-5}$, $I_{CDW}^C = 1.02 \times 10^{-5}$ and $I_{CDW}^D = 2.82 \times 10^{-6}$ at $k_B T / \Delta = 1/10$ for the three types of

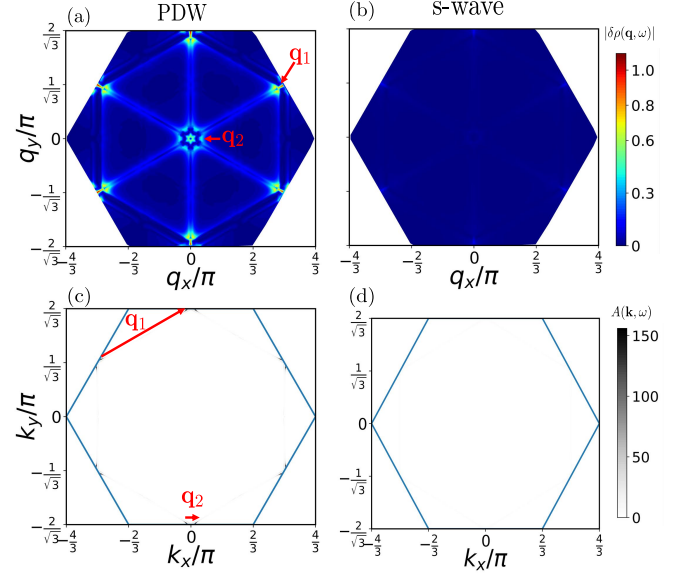


FIG. 4. LDOS modulation $|\delta\rho(\mathbf{q}, \omega)|$ for (a) the PDW state and (b) a uniform s-wave SC state. Electron spectral function $A(\mathbf{k}, \omega)$ for (c) the PDW state and (d) a uniform s-wave state. Wave vectors \mathbf{q}_1 and \mathbf{q}_2 in (a) and (c) indicate dominant scattering processes connecting two points with large $A(\mathbf{k}, \omega)$ (and their symmetric equivalence). Here $\omega = 0.01 < \Delta = 0.02$ has been chosen.

CDW wave vectors respectively.

Quasi-particle interference. — In the presence of elastic scatterings, the LDOS will be modulated due to the effect of QPI. To characterize this feature, we follow Ref. [39] to study the modulated LDOS $\delta\rho(\mathbf{r}, \omega)$, or its Fourier transformation $\delta\rho(\mathbf{q}, \omega)$ that is given by

$$\begin{aligned} \delta\rho(\mathbf{q}, \omega) &\equiv \rho_s(\mathbf{q}, \omega) - \rho(\mathbf{q}, \omega) \\ &= -\frac{1}{16\pi N} \sum_{\mathbf{k}} \text{Im} \tilde{\text{Tr}} \left[\hat{\mathcal{G}}(\mathbf{k} + \mathbf{q}, \omega + i\delta) \hat{T}(\omega) \hat{\mathcal{G}}(\mathbf{k}, \omega + i\delta) \right], \end{aligned} \quad (9)$$

where $\rho_s(\mathbf{q}, \omega)$ ($\rho(\mathbf{q}, \omega)$) is the LDOS in \mathbf{q} space in the presence (absence) of scatterings. $\tilde{\text{Tr}}$ means tracing the upper-left 16×16 block in a 32×32 matrix. $\hat{\mathcal{G}}(\mathbf{k}, \omega + i\delta)$ is Green's function in the absence of scatterings and $\hat{T}(\omega)$ is the scattering matrix, which are given by $\hat{\mathcal{G}}^{-1}(\mathbf{k}, \omega + i\delta) = (\omega + i\delta)I - \hat{\mathcal{H}}_{\mathbf{k}}$ and $\hat{T}^{-1}(\omega) = (V_s \hat{\tau}_3)^{-1} - \frac{1}{N} \sum_{\mathbf{k}} \hat{\mathcal{G}}(\mathbf{k}, \omega + i\delta)$ respectively. Here V_s is the nonmagnetic scattering impurity strength, and $\hat{\tau}_3$ is the Pauli matrix spanning Nambu space.

The modulation $|\delta\rho(\mathbf{q}, \omega)|$ with $V_s = 0.1$ at $\omega = 0.01 (< \Delta = 0.02)$ is plotted in Fig. 4(a). For comparison, we also study QPI of a uniform s-wave superconductor with gap $\Delta_s(\mathbf{k}) = \Delta \exp[-(|\xi_{\mathbf{k}}| + |\xi_{-\mathbf{k}}|)/(2\Delta)]$, as shown in Fig. 4(b). In both figures the intensity at $\mathbf{q} = \mathbf{0}$ has been subtracted.

Electron spectral function. — The LDOS modulation due to scatterings can be analyzed by electron spectral function $A(\mathbf{k}, \omega)$ in the absence of scattering. For our commensurate PDW state, $A(\mathbf{k}, \omega) = -\frac{1}{\pi} \text{Im}[\hat{\mathcal{G}}(\mathbf{k}, \omega + i\delta)]_{11}$. As is pointed out in Ref. [39], the \mathbf{k} -summation in Eq. (9) is dominated by terms in which both \mathbf{k} and $\mathbf{k} + \mathbf{q}$ are poles of $\hat{\mathcal{G}}$. Thus the

vectors \mathbf{q} associated with the scattering processes connecting two points with large $A(\mathbf{k}, \omega)$ will show significant $|\delta\rho(\mathbf{q}, \omega)|$. This feature of \mathbf{q} is displayed in Fig. 4(c). An essential difference between the PDW state and a uniform s-wave state is that in-gap state is absent in the latter and the corresponding $A(\mathbf{k}, \omega)$ and $|\delta\rho(\mathbf{q}, \omega)|$ approach to zero at $\omega < \Delta$, as shown in Fig. 4(b) and (d). This also provides an experiment scheme to probe PDW states.

Discussions and conclusions. —

(i) Recently discovered Kagome SC AV_3Sb_5 ($A=\text{K}, \text{Rb}, \text{Cs}$) with a nearly 3/4 filled electron band is a natural platform towards the realization of the interplay between PDW and FS nesting [40–43]. And the TRS breaking signatures have been extensively discussed both experimentally and theoretically in AV_3Sb_5 [44–49], which gives rise to a prerequisite to PDW formation. For the SC properties, the AV_3Sb_5 is shown to be a spin-singlet SC hosting conventional s-wave features [50–52]. However, a residual thermal transport at $T = 0$ and “multi-gap” V-shape DOS with residual zero-energy contributions were observed in the SC states [34, 52–54], which conflicts with the conventional s-wave nature. This contradiction can be resolved within the TRS breaking PDW scenario proposed in the present work. More importantly, a PDW state ordering at \mathbf{Q}_α has been observed in recent low-temperature high-resolution STM measurements [34]. Therefore, our theory may provide new insight into the PDW states and TRS breaking in AV_3Sb_5 . Indeed, both 2×2 and 4×4 CDW have been observed in STM. Our theory suggests that the $\frac{4}{\sqrt{3}} \times \frac{4}{\sqrt{3}}$ CDW should appear as well, as long as the frequency ω is chosen properly, although its integrated intensity is order of magnitude smaller than the other two.

(ii) Indeed, such a TRS breaking SC state breaks the spatial inversion symmetry as well, resulting in a chiral state with stable residual gapless Bogolubov quasi-particle excitation. This can be seen from Eq. (2).

(iii) One of remaining issues is what microscopic theory may give rise to the Cooper pairing instability at a finite momentum on a nested FS. In the weak interaction limit, pairing at zero momentum is usually favored. Nonetheless, strong correlation might favor PDW instability against uniform pairing (see, e.g. Ref.[15]).

(iv) In summary, we have found that the FS nesting allows a full PDW pairing and the existence of in-gap states simultaneously. Such a PDW ansatz will give rise to a TRS breaking ground state in the principle of energy minimization. Subsequently, descendant CDW orders, Bogoliubov Fermi pockets, DOS and LDOS, and the effect of QPI have been studied, and the relevance to newly discovered Kagome SC AV_3Sb_5 ($A=\text{K}, \text{Rb}, \text{Cs}$) has been revealed.

Acknowledgment.— We thank Hui Chen, Shiyan Li, Zheng Li, Tao Wu, Fu-Chun Zhang, and Tong Zhang for helpful discussions. This work is partially supported by National Natural Science Foundation of China (No. 12034004, No. 11774306, and No. 11825404) and the Strategic Priority Research Program of Chinese Academy of Sciences (No. XDB28000000).

* jiangkun@iphy.ac.cn

† yaohong@tsinghua.edu.cn

‡ yizhou@iphy.ac.cn

- [1] E. Berg, E. Fradkin, E.-A. Kim, S. A. Kivelson, V. Oganesyan, J. M. Tranquada, and S. C. Zhang, *Phys. Rev. Lett.* **99**, 127003 (2007).
- [2] D. Agterberg and H. Tsunetsugu, *Nature Physics* **4**, 639 (2008).
- [3] E. Berg, E. Fradkin, S. A. Kivelson, and J. M. Tranquada, *New Journal of Physics* **11**, 115004 (2009).
- [4] E. Berg, E. Fradkin, and S. A. Kivelson, *Phys. Rev. Lett.* **105**, 146403 (2010).
- [5] A. Jaefari and E. Fradkin, *Phys. Rev. B* **85**, 035104 (2012).
- [6] G. Y. Cho, J. H. Bardarson, Y.-M. Lu, and J. E. Moore, *Phys. Rev. B* **86**, 214514 (2012).
- [7] R. Soto-Garrido and E. Fradkin, *Phys. Rev. B* **89**, 165126 (2014).
- [8] P. A. Lee, *Phys. Rev. X* **4**, 031017 (2014).
- [9] J. Maciejko and R. Nandkishore, *Phys. Rev. B* **90**, 035126 (2014).
- [10] Y. Wang, D. F. Agterberg, and A. Chubukov, *Phys. Rev. Lett.* **114**, 197001 (2015).
- [11] S.-K. Jian, Y.-F. Jiang, and H. Yao, *Phys. Rev. Lett.* **114**, 237001 (2015).
- [12] S.-K. Jian, C.-H. Lin, J. Maciejko, and H. Yao, *Phys. Rev. Lett.* **118**, 166802 (2017).
- [13] Y. Wang, S. D. Edkins, M. H. Hamidian, J. C. S. Davis, E. Fradkin, and S. A. Kivelson, *Phys. Rev. B* **97**, 174510 (2018).
- [14] J. Venderley and E.-A. Kim, *Science advances* **5**, eaat4698 (2019).
- [15] Z. Han, S. A. Kivelson, and H. Yao, *Phys. Rev. Lett.* **125**, 167001 (2020).
- [16] K. Slagle and L. Fu, *Phys. Rev. B* **102**, 235423 (2020).
- [17] S. Zhou and Z. Wang, (2021), [arXiv:2110.06266](https://arxiv.org/abs/2110.06266) [cond-mat.supr-con].
- [18] K. S. Huang, Z. Han, S. A. Kivelson, and H. Yao, *npj Quantum Materials* **7**, 17 (2022).
- [19] Y.-M. Wu, Z. Wu, and H. Yao, [arXiv:2203.05480](https://arxiv.org/abs/2203.05480) (2022).
- [20] D. F. Agterberg, J. S. Davis, S. D. Edkins, E. Fradkin, D. J. Van Harlingen, S. A. Kivelson, P. A. Lee, L. Radzihovsky, J. M. Tranquada, and Y. Wang, *Annual Review of Condensed Matter Physics* **11**, 231 (2020).
- [21] P. Fulde and R. A. Ferrell, *Phys. Rev.* **135**, A550 (1964).
- [22] A. I. Larkin and Y. N. Ovchinnikov, *Sov. Phys. JETP* **28**, 1200 (1969).
- [23] R. Casalbuoni and G. Nardulli, *Rev. Mod. Phys.* **76**, 263 (2004).
- [24] M. H. Hamidian, S. D. Edkins, S. H. Joo, A. Kostin, H. Eisaki, S. Uchida, M. J. Lawler, E.-A. Kim, A. P. Mackenzie, K. Fujita, J. Lee, and J. C. S. Davis, *Nature* **532**, 343 (2016).
- [25] W. Ruan, X. Li, C. Hu, Z. Hao, H. Li, P. Cai, X. Zhou, D.-H. Lee, and Y. Wang, *Nature Physics* **14**, 1178 (2018).
- [26] S. D. Edkins, A. Kostin, K. Fujita, A. P. Mackenzie, H. Eisaki, S. Uchida, S. Sachdev, M. J. Lawler, E.-A. Kim, J. C. S. Davis, and M. H. Hamidian, *Science* **364**, 976 (2019), <https://www.science.org/doi/pdf/10.1126/science.aat1773>.
- [27] X. Li, C. Zou, Y. Ding, H. Yan, S. Ye, H. Li, Z. Hao, L. Zhao, X. Zhou, and Y. Wang, *Phys. Rev. X* **11**, 011007 (2021).
- [28] R. E. Peierls, *Quantum Theory of Solids* ((Oxford University, New York/London), 1955).
- [29] H. Fröhlich, *Proceedings of the Royal Society of London. Series A. Mathematical and Physical Sciences* **223**, 296 (1954).
- [30] G. Grüner, *Rev. Mod. Phys.* **60**, 1129 (1988).

- [31] A. W. Overhauser, [Phys. Rev. Lett. **4**, 462 \(1960\)](#).
- [32] A. W. Overhauser, [Phys. Rev. **128**, 1437 \(1962\)](#).
- [33] G. Grüner, [Rev. Mod. Phys. **66**, 1 \(1994\)](#).
- [34] H. Chen, H. Yang, B. Hu, Z. Zhao, J. Yuan, Y. Xing, G. Qian, Z. Huang, G. Li, Y. Ye, S. Ma, S. Ni, H. Zhang, Q. Yin, C. Gong, Z. Tu, H. Lei, H. Tan, S. Zhou, C. Shen, X. Dong, B. Yan, Z. Wang, and H.-J. Gao, [Nature **599**, 222 \(2021\)](#).
- [35] See the Supplemental Material for more details.
- [36] J. R. Schrieffer, *Theory of Superconductivity* (Westview Press, 1999).
- [37] G. Binnig and H. Rohrer, [Rev. Mod. Phys. **59**, 615 \(1987\)](#).
- [38] L. Van Hove, [Phys. Rev. **89**, 1189 \(1953\)](#).
- [39] Q.-H. Wang and D.-H. Lee, [Phys. Rev. B **67**, 020511 \(2003\)](#).
- [40] B. R. Ortiz, S. M. L. Teicher, Y. Hu, J. L. Zuo, P. M. Sarte, E. C. Schueller, A. M. M. Abeykoon, M. J. Krogstad, S. Rosenkranz, R. Osborn, R. Seshadri, L. Balents, J. He, and S. D. Wilson, [Phys. Rev. Lett. **125**, 247002 \(2020\)](#).
- [41] B. R. Ortiz, P. M. Sarte, E. M. Kenney, M. J. Graf, S. M. L. Teicher, R. Seshadri, and S. D. Wilson, [Phys. Rev. Materials **5**, 034801 \(2021\)](#).
- [42] Q. Yin, Z. Tu, C. Gong, Y. Fu, S. Yan, and H. Lei, [Chinese Physics Letters **38**, 037403 \(2021\)](#).
- [43] K. Jiang, T. Wu, J.-X. Yin, Z. Wang, M. Z. Hasan, S. D. Wilson, X. Chen, and J. Hu, (2021), [arXiv:2109.10809 \[cond-mat.supr-con\]](#).
- [44] Y.-X. Jiang, J.-X. Yin, M. M. Denner, N. Shumiya, B. R. Ortiz, G. Xu, Z. Guguchia, J. He, M. S. Hossain, X. Liu, and et al., [Nature Materials **20**, 1353 \(2021\)](#).
- [45] L. Yu, C. Wang, Y. Zhang, M. Sander, S. Ni, Z. Lu, S. Ma, Z. Wang, Z. Zhao, H. Chen, K. Jiang, Y. Zhang, H. Yang, F. Zhou, X. Dong, S. L. Johnson, M. J. Graf, J. Hu, H.-J. Gao, and Z. Zhao, (2021), [arXiv:2107.10714 \[cond-mat.supr-con\]](#).
- [46] C. M. I. au2, D. Das, J. X. Yin, H. Liu, R. Gupta, Y. X. Jiang, M. Medarde, X. Wu, H. C. Lei, J. J. Chang, P. Dai, Q. Si, H. Miao, R. Thomale, T. Neupert, Y. Shi, R. Khasanov, M. Z. Hasan, H. Luetkens, and Z. Guguchia, (2021), [arXiv:2106.13443 \[cond-mat.mtrl-sci\]](#).
- [47] X. Feng, K. Jiang, Z. Wang, and J. Hu, [Science Bulletin **66**, 1384 \(2021\)](#).
- [48] Y.-P. Lin and R. M. Nandkishore, [Phys. Rev. B **104**, 045122 \(2021\)](#).
- [49] T. Park, M. Ye, and L. Balents, [Phys. Rev. B **104**, 035142 \(2021\)](#).
- [50] C. Mu, Q. Yin, Z. Tu, C. Gong, H. Lei, Z. Li, and J. Luo, [Chin. Phys. Lett. **38**, 077402 \(2021\)](#).
- [51] W. Duan, Z. Nie, S. Luo, F. Yu, B. R. Ortiz, L. Yin, H. Su, F. Du, A. Wang, Y. Chen, X. Lu, J. Ying, S. D. Wilson, X. Chen, Y. Song, and H. Yuan, [Science China Physics, Mechanics & Astronomy **64**, 107462 \(2021\)](#).
- [52] H.-S. Xu, Y.-J. Yan, R. Yin, W. Xia, S. Fang, Z. Chen, Y. Li, W. Yang, Y. Guo, and D.-L. Feng, [Phys. Rev. Lett. **127**, 187004 \(2021\)](#).
- [53] C. C. Zhao, L. S. Wang, W. Xia, Q. W. Yin, J. M. Ni, Y. Y. Huang, C. P. Tu, Z. C. Tao, Z. J. Tu, C. S. Gong, H. C. Lei, Y. F. Guo, X. F. Yang, and S. Y. Li, (2021), [arXiv:2102.08356 \[cond-mat.supr-con\]](#).
- [54] Z. Liang, X. Hou, F. Zhang, W. Ma, P. Wu, Z. Zhang, F. Yu, J.-J. Ying, K. Jiang, L. Shan, Z. Wang, and X.-H. Chen, [Phys. Rev. X **11**, 031026 \(2021\)](#).

Supplementary Material for "Interplay between Pair Density Wave and a Nested Fermi Surface"

This supplementary Material provides more details on our hexagonal lattice model, including the proof of \mathbb{Z}_2 symmetry theorem, the calculation of $E(\mathbf{k})_1^+$ along the FS segment, more numerical study on the condensation energy, ground state degeneracy and the derivation of Ginzburg-Landau free energy and local density of states.

I. THE PROOF OF \mathbb{Z}_2 SYMMETRY THEOREM

Here we provide more details for the proof of the \mathbb{Z}_2 theorem presented in the main text.

Theorem: For each α , the transformation $\Delta_{\pm\mathbf{Q}_\alpha} \mapsto -\Delta_{\pm\mathbf{Q}_\alpha}$ does not change the energy spectra of the system.

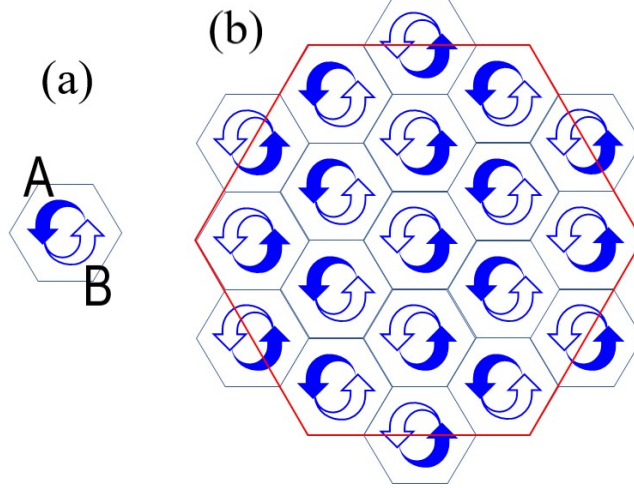


FIG. S1. (a) A centrosymmetric bipartition for the 4×4 folded BZ. The folded zone is divided into two parts A and B, such that A is the inversion of B. (b) A \mathbf{Q}_1 stripy tiling of the reciprocal plane with folded zone and its inversion. They are aligned alternatively along \mathbf{Q}_2 and \mathbf{Q}_3 directions, while keep \mathbf{Q}_1 translational invariant. This tiling gives rise to a centrosymmetric bipartition for the whole BZ, such that \mathbf{k} and $\mathbf{Q}_1 - \mathbf{k}$ belong to opposite parts (A and B), while $\mathbf{Q}_2 - \mathbf{k}$ and $\mathbf{Q}_3 - \mathbf{k}$ belong to the same part. The red hexagon encloses first (unfolded) BZ.

Proof: Without loss of generality, we consider $\alpha = 1$ and a centrosymmetric bipartition (A and B) of first BZ as illustrated in Fig. S1. Define a function $\eta(\mathbf{k}) := +(-)1$ for $\mathbf{k} \in A(B)$, we have $\eta(\mathbf{Q}_2 - \mathbf{k}) = \eta(\mathbf{Q}_3 - \mathbf{k}) = -\eta(\mathbf{Q}_1 - \mathbf{k}) = \eta(\mathbf{k})$. Thus, the unitary transformation: $c_{\mathbf{k},\uparrow} \mapsto c_{\mathbf{k},\uparrow}$ and $c_{\mathbf{k},\downarrow} \mapsto \eta(\mathbf{k})c_{\mathbf{k},\downarrow}$ gives rise to $\Delta_{\pm\mathbf{Q}_1} \mapsto -\Delta_{\pm\mathbf{Q}_1}$ and $\Delta_{\pm\mathbf{Q}_{2,3}} \mapsto \Delta_{\pm\mathbf{Q}_{2,3}}$, and will not change energy spectra. QED.

II. $E(\mathbf{k})_1^+$ ALONG THE HEXAGONAL FERMI SURFACE

We now study the approximate $E(\mathbf{k})_1^+$ along the FS. By symmetry, we consider the FS segment $M - X$ [see Figs. 1(a) and 1(b) in the main text] only. For \mathbf{k} satisfies $k_x = \pi$ and $k_y \in \left(0, \frac{\pi}{\sqrt{3}}\right)$, with sufficiently small energy cutoff Λ , the decomposition of $\hat{\mathcal{H}}_{\mathbf{k}}$ in Eq. (3b) is of the following form,

$$H_{\mathbf{k}} = \left(\hat{C}_{\mathbf{k},\uparrow}^{\dagger p}, \hat{C}_{-\mathbf{k},\downarrow}^p \right) \hat{\mathcal{H}}_{\mathbf{k}}^p \begin{pmatrix} \hat{C}_{\mathbf{k},\uparrow}^p \\ \hat{C}_{-\mathbf{k},\downarrow}^{\dagger p} \end{pmatrix} + \left(\hat{C}_{\mathbf{k},\uparrow}^{\dagger f}, \hat{C}_{-\mathbf{k},\downarrow}^f \right) \hat{\mathcal{H}}_{\mathbf{k}}^f \begin{pmatrix} \hat{C}_{\mathbf{k},\uparrow}^f \\ \hat{C}_{-\mathbf{k},\downarrow}^{\dagger f} \end{pmatrix}, \quad (\text{S1a})$$

where the pairing part $\hat{\mathcal{H}}_{\mathbf{k}}^p$ can be further decomposed as

$$\left(\hat{C}_{\mathbf{k},\uparrow}^{\dagger p}, \hat{C}_{-\mathbf{k},\downarrow}^p \right) \hat{\mathcal{H}}_{\mathbf{k}}^p \begin{pmatrix} \hat{C}_{\mathbf{k},\uparrow}^p \\ \hat{C}_{-\mathbf{k},\downarrow}^{\dagger p} \end{pmatrix} = \left(c_{\mathbf{k},\uparrow}^{\dagger}, c_{\mathbf{k}+2\mathbf{Q}_1,\uparrow}^{\dagger}, c_{-\mathbf{k}+\mathbf{Q}_1,\downarrow}, c_{-\mathbf{k}-\mathbf{Q}_1,\downarrow} \right) \hat{\mathcal{H}}_{\mathbf{k}}^{\bar{p}} \begin{pmatrix} c_{\mathbf{k},\uparrow} \\ c_{\mathbf{k}+2\mathbf{Q}_1,\uparrow} \\ c_{-\mathbf{k}+\mathbf{Q}_1,\downarrow}^{\dagger} \\ c_{-\mathbf{k}-\mathbf{Q}_1,\downarrow}^{\dagger} \end{pmatrix} + \left(c_{\mathbf{k}+\mathbf{Q}_1,\uparrow}^{\dagger}, c_{\mathbf{k}-\mathbf{Q}_1,\uparrow}^{\dagger}, c_{-\mathbf{k},\downarrow}, c_{-\mathbf{k}+2\mathbf{Q}_1,\downarrow} \right) \hat{\mathcal{H}}_{\mathbf{k}}^{\bar{p}} \begin{pmatrix} c_{\mathbf{k}+\mathbf{Q}_1,\uparrow} \\ c_{\mathbf{k}-\mathbf{Q}_1,\uparrow} \\ c_{-\mathbf{k},\downarrow}^{\dagger} \\ c_{-\mathbf{k}+2\mathbf{Q}_1,\downarrow}^{\dagger} \end{pmatrix}.$$

Here $\hat{\mathcal{H}}_{\mathbf{k}}^{\tilde{p}}$ reads

$$\hat{\mathcal{H}}_{\mathbf{k}}^{\tilde{p}} = \begin{pmatrix} 0 & 0 & \Delta_{\mathbf{Q}_1} & \Delta_{-\mathbf{Q}_1} \\ 0 & 0 & \Delta_{-\mathbf{Q}_1} & \Delta_{\mathbf{Q}_1} \\ \Delta_{\mathbf{Q}_1}^* & \Delta_{-\mathbf{Q}_1}^* & 0 & 0 \\ \Delta_{-\mathbf{Q}_1}^* & \Delta_{\mathbf{Q}_1}^* & 0 & 0 \end{pmatrix} = \Delta \begin{pmatrix} 0 & 0 & e^{i\frac{\phi_1}{2} + i\theta_1} & e^{-i\frac{\phi_1}{2} + i\theta_1} \\ 0 & 0 & e^{-i\frac{\phi_1}{2} + i\theta_1} & e^{i\frac{\phi_1}{2} + i\theta_1} \\ e^{-i\frac{\phi_1}{2} - i\theta_1} & e^{i\frac{\phi_1}{2} - i\theta_1} & 0 & 0 \\ e^{i\frac{\phi_1}{2} - i\theta_1} & e^{-i\frac{\phi_1}{2} - i\theta_1} & 0 & 0 \end{pmatrix}. \quad (\text{S1b})$$

$$\hat{\mathcal{C}}_{\mathbf{k},\uparrow}^{\dagger f} = (c_{\mathbf{k}+\mathbf{Q}_2,\uparrow}^{\dagger}, c_{\mathbf{k}-\mathbf{Q}_2,\uparrow}^{\dagger}, c_{\mathbf{k}+\mathbf{Q}_3,\uparrow}^{\dagger}, c_{\mathbf{k}-\mathbf{Q}_3,\uparrow}^{\dagger}, c_{\mathbf{k}+2\mathbf{Q}_2,\uparrow}^{\dagger}, c_{\mathbf{k}+2\mathbf{Q}_3,\uparrow}^{\dagger}, c_{\mathbf{k}+\mathbf{Q}_1-\mathbf{Q}_2,\uparrow}^{\dagger}, c_{\mathbf{k}-\mathbf{Q}_1+\mathbf{Q}_2,\uparrow}^{\dagger}, c_{\mathbf{k}+\mathbf{Q}_2-\mathbf{Q}_3,\uparrow}^{\dagger}, c_{\mathbf{k}-\mathbf{Q}_2+\mathbf{Q}_3,\uparrow}^{\dagger}, c_{\mathbf{k}+\mathbf{Q}_3-\mathbf{Q}_1,\uparrow}^{\dagger}, c_{\mathbf{k}-\mathbf{Q}_3+\mathbf{Q}_1,\uparrow}^{\dagger}) \text{ and}$$

$$\hat{\mathcal{H}}_{\mathbf{k}}^f = \begin{pmatrix} \hat{D}^f(\mathbf{k}) & 0 \\ 0 & -\hat{D}^f(-\mathbf{k}) \end{pmatrix}, \quad (\text{S1c})$$

where $\hat{D}^f(\mathbf{k}) = \text{diag}\{\xi_{\mathbf{k}_i^f}\}$ is a diagonal matrix and \mathbf{k}_i^f is the i -th momentum in $\hat{\mathcal{C}}_{\mathbf{k},\uparrow}^{\dagger f}$.

We define $E^p(\mathbf{k})$ and $E^f(\mathbf{k})$ as the lowest non-negative eigenvalues of $\hat{\mathcal{H}}_{\mathbf{k}}^p$ and $\hat{\mathcal{H}}_{\mathbf{k}}^f$ respectively. The eigenvalues of Eq. (S1b) are $\pm 2\Delta \sin(\frac{\phi_1}{2})$ and $\pm 2\Delta \cos(\frac{\phi_1}{2})$. Thus $E^p(\mathbf{k}) = 2\Delta \min\left\{\left|\sin\left(\frac{\phi_1}{2}\right)\right|, \left|\cos\left(\frac{\phi_1}{2}\right)\right|\right\}$. From Eq. (S1c), we obtain that $E^f(\mathbf{k}) = \min\{|\xi_{\mathbf{k}_i^f}|\}$. Hence we have

$$E(\mathbf{k})_1^+ \approx \min\{E^p(\mathbf{k}), E^f(\mathbf{k})\} = \min\left\{2\Delta \min\left\{\left|\sin\left(\frac{\phi_1}{2}\right)\right|, \left|\cos\left(\frac{\phi_1}{2}\right)\right|\right\}, \min\{|\xi_{\mathbf{k}_i^f}|\}\right\}. \quad (\text{S2})$$

Notice that the eigenvalues of Eq. (S1b) and Eq. (S1c) are θ_α -independent. To study the effect of TRS breaking, we need to consider pairing along all the three directions of \mathbf{Q}_α numerically.

III. NUMERICAL STUDY ON CONDENSATION ENERGY

To show that the aforementioned approximation of $E(\mathbf{k})_1^+$ is reasonable and E_c acquires local maxima at $\phi_\alpha = \pm\pi/2$, we study E_c at different ϕ_α numerically, keeping $\Delta = 0.02$ and $\Lambda = 0.1$. We fix the values of θ_α randomly and find ϕ_α that maximize E_c . For various random initial variables ϕ_α , the results that maximize the condensation energy fit $\phi_\alpha = \pm\pi/2$ well.

Here we present a numerical result of a special case: keeping $\theta_\alpha = 0, 2\pi/3, -2\pi/3$ and setting $\phi_1 = \phi_2 = \phi_3 = \phi$. The result of $E_c(\phi)$ is shown in Fig. S2. We can see that the maximum of $E_c(\phi)$ is found at $\phi = \pm\pi/2$, which is in good agreement with our analysis of approximate $E(\mathbf{k})_1^+$.

To further check our results, we maximize the condensation energy $E_c[\theta_2, \theta_3, \phi_\alpha]$ numerically, keeping $\theta_1 = 0, \Delta = 0.02$ and $\Lambda = 0.1$. For various random initial variables $[\theta_2, \theta_3, \phi_\alpha]$, the results that maximize the condensation energy fit $\phi_\alpha = \pm\pi/2$ and $\theta_2 - \theta_1 = \theta_3 - \theta_2 \equiv \pm 2\pi/3 \pmod{\pi}$ well.

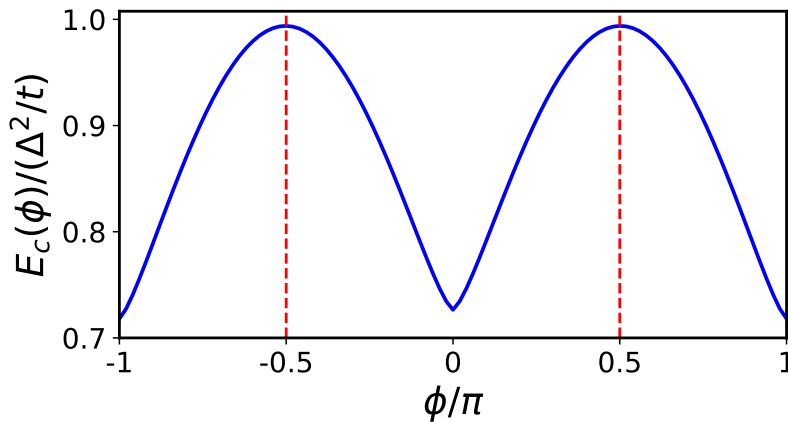


FIG. S2. Condensation energy E_c as a function of ϕ . Here $\theta_1 = 0, \theta_2 = 2\pi/3, \theta_3 = -2\pi/3, \phi_1 = \phi_2 = \phi_3 = \phi, \Delta = 0.02$ and $\Lambda = 0.1$ have been chosen.

IV. GROUND STATE DEGENERACY

Since the condensation energy is maximized at $\phi_\alpha = \pm\pi/2$ and $\theta_2 - \theta_1 = \theta_3 - \theta_2 \equiv \pm 2\pi/3 \pmod{\pi}$, each set of $[\theta_\alpha, \phi_\alpha]$ satisfies these conditions will give rise to a ground state of the system. We now discuss the ground state degeneracy of our PDW state. Notice that a gauge transformation reads $c_{\mathbf{r},\sigma} \mapsto e^{i\theta_1/2} c_{\mathbf{r},\sigma}$ leads to a transformation of θ_α as follows,

$$[\theta_1, \theta_2, \theta_3] \mapsto [0, \theta_2 - \theta_1, \theta_3 - \theta_1].$$

Thus, we can always set $\theta_1 = 0$ and focus on different sets of $[\theta_2, \theta_3, \phi_\alpha]$ satisfy $\phi_\alpha = \pm\pi/2$ and $\theta_2 = \theta_3 - \theta_2 \equiv \pm 2\pi/3 \pmod{\pi}$. There are 8 sets of $[\theta_2, \theta_3]$ satisfy $\theta_2 = \theta_3 - \theta_2 \equiv \pm 2\pi/3 \pmod{\pi}$ (it can be seen from the 8 maxima in Fig. 2(a) in the main text) and 8 sets of $[\phi_1, \phi_2, \phi_3]$ satisfy $\phi_\alpha = \pm\pi/2$. Consequently, the ground state is of 8×8 -fold degeneracy.

The 64 different ground states can be related through several symmetry operators. It can be seen from the transformation of $\Delta(\mathbf{r})$ under the corresponding symmetry operator. Recall the form of $\Delta(\mathbf{r})$ in Eq. (2),

$$\Delta(\mathbf{r}) = 2\Delta \sum_{\alpha} e^{i\theta_{\alpha}} \cos\left(\mathbf{Q}_{\alpha} \cdot \mathbf{r} + \frac{\phi_{\alpha}}{2}\right).$$

The \mathbb{Z}_2 transformation $\Delta_{\pm\mathbf{Q}_{\alpha}} \mapsto -\Delta_{\pm\mathbf{Q}_{\alpha}}$ gives rise to $\theta_{\alpha} \mapsto \theta_{\alpha} + \pi$ (for a certain α). The time reversal transformation leads to $\Delta(\mathbf{r}) \mapsto \Delta^*(\mathbf{r})$ as well as $\theta_{\alpha} \mapsto -\theta_{\alpha}$ (acting on all the three α simultaneously). Thus the 8 sets of $[\theta_2, \theta_3]$ can be related with each other through these two kinds of transformations. As for the 8 sets of $[\phi_1, \phi_2, \phi_3]$, we can apply the lattice translation operator: $T_i : \mathbf{r} \mapsto \mathbf{r} + \mathbf{a}_i$ ($\mathbf{Q}_i \cdot \mathbf{a}_j = \pi/2\delta_{ij}$, $i, j = 1, 2$), the spatial inversion operator $\mathcal{P} : \mathbf{r} \mapsto -\mathbf{r}$ and the \mathbb{Z}_2 transformation to change the sign of one ϕ_{α} and keep the other two unchanged. This process provides a path links two sets of $[\phi_1, \phi_2, \phi_3]$ and all the 8 sets of $[\phi_1, \phi_2, \phi_3]$ are related with each other through these paths. As a concrete example, we give the specific process of the transformation $[\pi/2, \pi/2, \pi/2] \mapsto [-\pi/2, \pi/2, \pi/2]$ here. Begin with $[\phi_1, \phi_2, \phi_3] = [\pi/2, \pi/2, \pi/2]$, $\Delta(\mathbf{r})$ is of the following form

$$\Delta_0(\mathbf{r}) = 2\Delta \left[\cos\left(\mathbf{Q}_1 \cdot \mathbf{r} + \frac{\pi}{4}\right) + e^{i\theta_2} \cos\left(\mathbf{Q}_2 \cdot \mathbf{r} + \frac{\pi}{4}\right) + e^{i\theta_3} \cos\left(\mathbf{Q}_3 \cdot \mathbf{r} + \frac{\pi}{4}\right) \right]. \quad (\text{S3a})$$

Under $T_2 : \mathbf{r} \mapsto \mathbf{r} + \mathbf{a}_2$, $\Delta(\mathbf{r})$ becomes

$$\Delta_0(\mathbf{r}) \mapsto \Delta_1(\mathbf{r}) = 2\Delta \left[\cos\left(\mathbf{Q}_1 \cdot \mathbf{r} + \frac{\pi}{4}\right) + e^{i\theta_2} \cos\left(\mathbf{Q}_2 \cdot \mathbf{r} + \frac{3\pi}{4}\right) + e^{i\theta_3} \cos\left(\mathbf{Q}_3 \cdot \mathbf{r} - \frac{\pi}{4}\right) \right]. \quad (\text{S3b})$$

Then the transformation $\Delta_{\pm\mathbf{Q}_2} \mapsto -\Delta_{\pm\mathbf{Q}_2}$ ($\theta_2 \mapsto \theta_2 + \pi$) gives rise to

$$\Delta_1(\mathbf{r}) \mapsto \Delta_2(\mathbf{r}) = 2\Delta \left[\cos\left(\mathbf{Q}_1 \cdot \mathbf{r} + \frac{\pi}{4}\right) + e^{i\theta_2} \cos\left(\mathbf{Q}_2 \cdot \mathbf{r} - \frac{\pi}{4}\right) + e^{i\theta_3} \cos\left(\mathbf{Q}_3 \cdot \mathbf{r} - \frac{\pi}{4}\right) \right]. \quad (\text{S3c})$$

Finally, we obtain $\Delta(\mathbf{r})$ with $[\phi_1, \phi_2, \phi_3] = [-\pi/2, \pi/2, \pi/2]$ under the operator \mathcal{P} ,

$$\Delta_2(\mathbf{r}) \mapsto \Delta_3(\mathbf{r}) = 2\Delta \left[\cos\left(\mathbf{Q}_1 \cdot \mathbf{r} - \frac{\pi}{4}\right) + e^{i\theta_2} \cos\left(\mathbf{Q}_2 \cdot \mathbf{r} + \frac{\pi}{4}\right) + e^{i\theta_3} \cos\left(\mathbf{Q}_3 \cdot \mathbf{r} + \frac{\pi}{4}\right) \right]. \quad (\text{S3d})$$

V. GINZBURG-LANDAU FREE ENERGY

We begin with the Gorkov Green's function $\mathcal{G}(i\omega_n, \mathbf{k})$ in our PDW state,

$$\mathcal{G}^{-1}(i\omega_n, \mathbf{k}) \equiv \mathcal{G}_0^{-1}(i\omega_n, \mathbf{k}) + \Sigma(\mathbf{k}), \quad (\text{S4})$$

where

$$\mathcal{G}_0^{-1}(i\omega_n, \mathbf{k}) = \begin{pmatrix} G_0^{-1}(i\omega_n, \mathbf{k}) & 0 \\ 0 & -G_0^{-1}(-i\omega_n, -\mathbf{k}) \end{pmatrix}, \quad \Sigma(\mathbf{k}) = \begin{pmatrix} 0 & -\hat{\Delta}(\mathbf{k}) \\ -\hat{\Delta}^{\dagger}(\mathbf{k}) & 0 \end{pmatrix}. \quad (\text{S5})$$

Here $G_0(i\omega_n, \mathbf{k})$ is the normal state Green's function. In our PDW state, $G_0(i\omega_n, \mathbf{k})$ is a 16×16 matrix satisfies $G_0(i\omega_n, \mathbf{k})_{ij} = (i\omega_n - \xi_{\mathbf{k}_i})^{-1} \delta_{ij}$ (\mathbf{k}_i is the i -th momentum in $\hat{\mathbf{C}}_{\mathbf{k},\uparrow}^{\dagger}$ in the main text). $\hat{\Delta}(\mathbf{k})$ is a 16×16 pairing matrix defined by $\Delta_{\pm\mathbf{Q}_{\alpha}}(\mathbf{k})$.

The mean-field free energy can be expressed as

$$\mathcal{F}[\Delta_{\pm\mathbf{Q}_{\alpha}}] \equiv -\frac{1}{16\beta} \sum_{n,\mathbf{k}} \text{Tr} \ln \mathcal{G}^{-1}(i\omega_n, \mathbf{k}) = \mathcal{F}^{(0)} - \frac{1}{16\beta} \sum_{n,\mathbf{k}} \text{Tr} \ln (1 + \mathcal{G}_0(i\omega_n, \mathbf{k}) \Sigma(\mathbf{k})) = \mathcal{F}^{(0)} + \sum_{j=1}^{\infty} \mathcal{F}^{(2j)}, \quad (\text{S6})$$

where $\mathcal{F}^{(0)}$ is a constant that is independent of $\Delta_{\pm\mathbf{Q}_\alpha}$. $\mathcal{F}^{(2j)}$ is the free energy of order $|\Delta_{\pm\mathbf{Q}_\alpha}|^{2j}$ of the following form,

$$\mathcal{F}^{(2j)} = \frac{1}{32j\beta} \sum_{n,\mathbf{k}} \text{Tr} \left[(\mathcal{G}_0(i\omega_n, \mathbf{k}) \Sigma(\mathbf{k}))^{2j} \right] = \frac{1}{16j\beta} \sum_{n,\mathbf{k}} \text{Tr} \left[\left(-G_0(i\omega_n, \mathbf{k}) \hat{\Delta}(\mathbf{k}) G_0(-i\omega_n, -\mathbf{k}) \hat{\Delta}^\dagger(\mathbf{k}) \right)^j \right]. \quad (\text{S7})$$

Notice that the factor $\frac{1}{16}$ comes from the 4×4 folding of the system and the summation over \mathbf{k} is performed in the first BZ.

For $j = 1$,

$$\mathcal{F}^{(2)} = -\frac{1}{16\beta} \sum_{n,\mathbf{k}} \text{Tr} \left[G_0(i\omega_n, \mathbf{k}) \hat{\Delta}(\mathbf{k}) G_0(-i\omega_n, -\mathbf{k}) \hat{\Delta}^\dagger(\mathbf{k}) \right] = \frac{1}{16\beta} \sum_{n,\mathbf{k},i} \frac{e^{-\frac{|\xi_{\mathbf{k}_i}|}{\Lambda}}}{i\omega_n - \xi_{\mathbf{k}_i}} a(i\omega_n, \mathbf{k}_i), \quad (\text{S8})$$

where Λ is the energy cutoff and

$$a(i\omega_n, \mathbf{k}_i) = \sum_{\alpha=1}^3 \left(\frac{e^{-\frac{|\xi_{-\mathbf{k}_i+\mathbf{Q}_\alpha}|}{\Lambda}}}{i\omega_n + \xi_{-\mathbf{k}_i+\mathbf{Q}_\alpha}} |\Delta_{\mathbf{Q}_\alpha}|^2 + \frac{e^{-\frac{|\xi_{-\mathbf{k}_i-\mathbf{Q}_\alpha}|}{\Lambda}}}{i\omega_n + \xi_{-\mathbf{k}_i-\mathbf{Q}_\alpha}} |\Delta_{-\mathbf{Q}_\alpha}|^2 \right). \quad (\text{S9})$$

By performing the summation over $i\omega_n$ and \mathbf{k} , we can obtain the following $\mathcal{F}^{(2)}$,

$$\mathcal{F}^{(2)} = g^{(2)} \sum_{\alpha=1}^3 \left(|\Delta_{\mathbf{Q}_\alpha}|^2 + |\Delta_{-\mathbf{Q}_\alpha}|^2 \right), \quad (\text{S10})$$

where $g^{(2)}$ is the corresponding coefficient.

For $j = 2$,

$$\mathcal{F}^{(4)} = \frac{1}{32\beta} \sum_{n,\mathbf{k}} \text{Tr} \left[\left(G_0(i\omega_n, \mathbf{k}) \hat{\Delta}(\mathbf{k}) G_0(-i\omega_n, -\mathbf{k}) \hat{\Delta}^\dagger(\mathbf{k}) \right)^2 \right] = \frac{1}{32\beta} \sum_{n,i,j} \sum_{\mathbf{k}}' \frac{1}{(i\omega_n - \xi_{\mathbf{k}_i})(i\omega_n - \xi_{\mathbf{k}_j})} b(i\omega_n, \mathbf{k}_i, \mathbf{k}_j), \quad (\text{S11})$$

where we introduce $\sum_{\mathbf{k}}'$ to represent the summation over \mathbf{k} with the energy cutoff as follows,

$$\sum_{\mathbf{k}}' \frac{1}{(i\omega_n - \xi_{\mathbf{k}_i})(i\omega_n - \xi_{\mathbf{k}_j})(i\omega_n + \xi_{\mathbf{k}_p})(i\omega_n + \xi_{\mathbf{k}_q})} = \sum_{\mathbf{k}} \frac{e^{-\frac{|\xi_{\mathbf{k}_i}|+|\xi_{\mathbf{k}_j}|+|\xi_{\mathbf{k}_p}|+|\xi_{\mathbf{k}_q}|}{\Lambda}}}{(i\omega_n - \xi_{\mathbf{k}_i})(i\omega_n - \xi_{\mathbf{k}_j})(i\omega_n + \xi_{\mathbf{k}_p})(i\omega_n + \xi_{\mathbf{k}_q})}. \quad (\text{S12})$$

Since the system is of 4×4 folded, we can keep $i = 1$ as well as $\mathbf{k}_i = \mathbf{k}$ and calculate the summation over j , $i\omega_n$ and \mathbf{k} . Then the summation over i will give rise to 16 copies. Thus, we can obtain the following $\mathcal{F}^{(4)}$ according to Eq. (S11),

$$\mathcal{F}^{(4)} = \frac{1}{2\beta} \sum_{n,j} \sum_{\mathbf{k}}' \frac{1}{(i\omega_n - \xi_{\mathbf{k}})(i\omega_n - \xi_{\mathbf{k}_j})} b(i\omega_n, \mathbf{k}, \mathbf{k}_j), \quad (\text{S13})$$

where $b(i\omega_n, \mathbf{k}, \mathbf{k}_j)$ reads

$$b(i\omega_n, \mathbf{k}, \mathbf{k}) = \left[\sum_{\alpha=1}^3 \left(\frac{|\Delta_{\mathbf{Q}_\alpha}|^2}{i\omega_n + \xi_{-\mathbf{k}+\mathbf{Q}_\alpha}} + \frac{|\Delta_{-\mathbf{Q}_\alpha}|^2}{i\omega_n + \xi_{-\mathbf{k}-\mathbf{Q}_\alpha}} \right) \right]^2, \quad (\text{S14a})$$

$$\begin{aligned} b(i\omega_n, \mathbf{k}, \mathbf{k} + \mathbf{Q}_1) &= \left(\frac{\Delta_{\mathbf{Q}_2} \Delta_{-\mathbf{Q}_3}^*}{i\omega_n + \xi_{-\mathbf{k}+\mathbf{Q}_2}} + \frac{\Delta_{\mathbf{Q}_3} \Delta_{-\mathbf{Q}_2}^*}{i\omega_n + \xi_{-\mathbf{k}+\mathbf{Q}_3}} \right) \left(\frac{\Delta_{-\mathbf{Q}_3} \Delta_{\mathbf{Q}_2}^*}{i\omega_n + \xi_{-\mathbf{k}+\mathbf{Q}_2}} + \frac{\Delta_{-\mathbf{Q}_2} \Delta_{\mathbf{Q}_3}^*}{i\omega_n + \xi_{-\mathbf{k}+\mathbf{Q}_3}} \right) \\ &= \frac{|\Delta_{\mathbf{Q}_2}|^2 |\Delta_{-\mathbf{Q}_3}|^2}{(i\omega_n + \xi_{-\mathbf{k}+\mathbf{Q}_2})^2} + \frac{|\Delta_{-\mathbf{Q}_2}|^2 |\Delta_{\mathbf{Q}_3}|^2}{(i\omega_n + \xi_{-\mathbf{k}+\mathbf{Q}_3})^2} + \frac{(\Delta_{\mathbf{Q}_2} \Delta_{-\mathbf{Q}_2})(\Delta_{\mathbf{Q}_3} \Delta_{-\mathbf{Q}_3})^* + c.c.}{(i\omega_n + \xi_{-\mathbf{k}+\mathbf{Q}_2})(i\omega_n + \xi_{-\mathbf{k}+\mathbf{Q}_3})}, \end{aligned} \quad (\text{S14b})$$

$$\begin{aligned} b(i\omega_n, \mathbf{k}, \mathbf{k} - \mathbf{Q}_1) &= \left(\frac{\Delta_{-\mathbf{Q}_2} \Delta_{\mathbf{Q}_3}^*}{i\omega_n + \xi_{-\mathbf{k}-\mathbf{Q}_2}} + \frac{\Delta_{-\mathbf{Q}_3} \Delta_{\mathbf{Q}_2}^*}{i\omega_n + \xi_{-\mathbf{k}-\mathbf{Q}_3}} \right) \left(\frac{\Delta_{\mathbf{Q}_3} \Delta_{-\mathbf{Q}_2}^*}{i\omega_n + \xi_{-\mathbf{k}-\mathbf{Q}_2}} + \frac{\Delta_{\mathbf{Q}_2} \Delta_{-\mathbf{Q}_3}^*}{i\omega_n + \xi_{-\mathbf{k}-\mathbf{Q}_3}} \right) \\ &= \frac{|\Delta_{-\mathbf{Q}_2}|^2 |\Delta_{\mathbf{Q}_3}|^2}{(i\omega_n + \xi_{-\mathbf{k}-\mathbf{Q}_2})^2} + \frac{|\Delta_{-\mathbf{Q}_3}|^2 |\Delta_{-\mathbf{Q}_2}|^2}{(i\omega_n + \xi_{-\mathbf{k}-\mathbf{Q}_3})^2} + \frac{(\Delta_{\mathbf{Q}_2} \Delta_{-\mathbf{Q}_2})(\Delta_{\mathbf{Q}_3} \Delta_{-\mathbf{Q}_3})^* + c.c.}{(i\omega_n + \xi_{-\mathbf{k}-\mathbf{Q}_2})(i\omega_n + \xi_{-\mathbf{k}-\mathbf{Q}_3})}, \end{aligned} \quad (\text{S14c})$$

$$\begin{aligned}
b(i\omega_n, \mathbf{k}, \mathbf{k} - \mathbf{Q}_1 + \mathbf{Q}_3) &= \left(\frac{\Delta_{\mathbf{Q}_1} \Delta_{\mathbf{Q}_3}^*}{i\omega_n + \xi_{-\mathbf{k}+\mathbf{Q}_1}} + \frac{\Delta_{-\mathbf{Q}_3} \Delta_{-\mathbf{Q}_1}^*}{i\omega_n + \xi_{-\mathbf{k}-\mathbf{Q}_3}} \right) \left(\frac{\Delta_{\mathbf{Q}_3} \Delta_{\mathbf{Q}_1}^*}{i\omega_n + \xi_{-\mathbf{k}+\mathbf{Q}_1}} + \frac{\Delta_{-\mathbf{Q}_1} \Delta_{-\mathbf{Q}_3}^*}{i\omega_n + \xi_{-\mathbf{k}-\mathbf{Q}_3}} \right) \\
&= \frac{|\Delta_{\mathbf{Q}_1}|^2 |\Delta_{\mathbf{Q}_3}|^2}{(i\omega_n + \xi_{-\mathbf{k}+\mathbf{Q}_1})^2} + \frac{|\Delta_{-\mathbf{Q}_1}|^2 |\Delta_{-\mathbf{Q}_3}|^2}{(i\omega_n + \xi_{-\mathbf{k}-\mathbf{Q}_3})^2} + \frac{(\Delta_{\mathbf{Q}_1} \Delta_{-\mathbf{Q}_1})(\Delta_{\mathbf{Q}_3} \Delta_{-\mathbf{Q}_3})^* + c.c.}{(i\omega_n + \xi_{-\mathbf{k}+\mathbf{Q}_1})(i\omega_n + \xi_{-\mathbf{k}-\mathbf{Q}_3})},
\end{aligned} \tag{S14n}$$

$$\begin{aligned}
b(i\omega_n, \mathbf{k}, \mathbf{k} + \mathbf{Q}_2 - \mathbf{Q}_3) &= \left(\frac{\Delta_{-\mathbf{Q}_2} \Delta_{-\mathbf{Q}_3}^*}{i\omega_n + \xi_{-\mathbf{k}-\mathbf{Q}_2}} + \frac{\Delta_{\mathbf{Q}_3} \Delta_{\mathbf{Q}_2}^*}{i\omega_n + \xi_{-\mathbf{k}+\mathbf{Q}_3}} \right) \left(\frac{\Delta_{-\mathbf{Q}_3} \Delta_{-\mathbf{Q}_2}^*}{i\omega_n + \xi_{-\mathbf{k}-\mathbf{Q}_2}} + \frac{\Delta_{\mathbf{Q}_2} \Delta_{\mathbf{Q}_3}^*}{i\omega_n + \xi_{-\mathbf{k}+\mathbf{Q}_3}} \right) \\
&= \frac{|\Delta_{-\mathbf{Q}_2}|^2 |\Delta_{-\mathbf{Q}_3}|^2}{(i\omega_n + \xi_{-\mathbf{k}-\mathbf{Q}_2})^2} + \frac{|\Delta_{\mathbf{Q}_2}|^2 |\Delta_{\mathbf{Q}_3}|^2}{(i\omega_n + \xi_{-\mathbf{k}+\mathbf{Q}_3})^2} + \frac{(\Delta_{\mathbf{Q}_2} \Delta_{-\mathbf{Q}_2})(\Delta_{\mathbf{Q}_3} \Delta_{-\mathbf{Q}_3})^* + c.c.}{(i\omega_n + \xi_{-\mathbf{k}-\mathbf{Q}_2})(i\omega_n + \xi_{-\mathbf{k}+\mathbf{Q}_3})},
\end{aligned} \tag{S14o}$$

$$\begin{aligned}
b(i\omega_n, \mathbf{k}, \mathbf{k} - \mathbf{Q}_2 + \mathbf{Q}_3) &= \left(\frac{\Delta_{\mathbf{Q}_2} \Delta_{\mathbf{Q}_3}^*}{i\omega_n + \xi_{-\mathbf{k}+\mathbf{Q}_2}} + \frac{\Delta_{-\mathbf{Q}_3} \Delta_{-\mathbf{Q}_2}^*}{i\omega_n + \xi_{-\mathbf{k}-\mathbf{Q}_3}} \right) \left(\frac{\Delta_{\mathbf{Q}_3} \Delta_{\mathbf{Q}_2}^*}{i\omega_n + \xi_{-\mathbf{k}+\mathbf{Q}_2}} + \frac{\Delta_{-\mathbf{Q}_2} \Delta_{-\mathbf{Q}_3}^*}{i\omega_n + \xi_{-\mathbf{k}-\mathbf{Q}_3}} \right) \\
&= \frac{|\Delta_{\mathbf{Q}_2}|^2 |\Delta_{\mathbf{Q}_3}|^2}{(i\omega_n + \xi_{-\mathbf{k}+\mathbf{Q}_2})^2} + \frac{|\Delta_{-\mathbf{Q}_2}|^2 |\Delta_{-\mathbf{Q}_3}|^2}{(i\omega_n + \xi_{-\mathbf{k}-\mathbf{Q}_3})^2} + \frac{(\Delta_{\mathbf{Q}_2} \Delta_{-\mathbf{Q}_2})(\Delta_{\mathbf{Q}_3} \Delta_{-\mathbf{Q}_3})^* + c.c.}{(i\omega_n + \xi_{-\mathbf{k}+\mathbf{Q}_2})(i\omega_n + \xi_{-\mathbf{k}-\mathbf{Q}_3})}.
\end{aligned} \tag{S14p}$$

By performing the summation over $i\omega_n$ and \mathbf{k} , $\mathcal{F}^{(4)}$ is of the following form,

$$\begin{aligned}
\mathcal{F}^{(4)} &= g_1^{(4)} \left(|\Delta_{\mathbf{Q}_1}|^4 + |\Delta_{-\mathbf{Q}_1}|^4 + |\Delta_{\mathbf{Q}_2}|^4 + |\Delta_{-\mathbf{Q}_2}|^4 + |\Delta_{\mathbf{Q}_3}|^4 + |\Delta_{-\mathbf{Q}_3}|^4 \right) \\
&+ g_2^{(4)} \left(|\Delta_{\mathbf{Q}_1}|^2 |\Delta_{-\mathbf{Q}_1}|^2 + |\Delta_{\mathbf{Q}_2}|^2 |\Delta_{-\mathbf{Q}_2}|^2 + |\Delta_{\mathbf{Q}_3}|^2 |\Delta_{-\mathbf{Q}_3}|^2 \right) \\
&+ g_3^{(4)} \left(|\Delta_{\mathbf{Q}_1}|^2 |\Delta_{\mathbf{Q}_2}|^2 + |\Delta_{\mathbf{Q}_2}|^2 |\Delta_{\mathbf{Q}_3}|^2 + |\Delta_{\mathbf{Q}_3}|^2 |\Delta_{\mathbf{Q}_1}|^2 + |\Delta_{-\mathbf{Q}_1}|^2 |\Delta_{-\mathbf{Q}_2}|^2 + |\Delta_{-\mathbf{Q}_2}|^2 |\Delta_{-\mathbf{Q}_3}|^2 + |\Delta_{-\mathbf{Q}_3}|^2 |\Delta_{-\mathbf{Q}_1}|^2 \right) \\
&+ g_4^{(4)} \left(|\Delta_{\mathbf{Q}_1}|^2 |\Delta_{-\mathbf{Q}_2}|^2 + |\Delta_{\mathbf{Q}_2}|^2 |\Delta_{-\mathbf{Q}_3}|^2 + |\Delta_{\mathbf{Q}_3}|^2 |\Delta_{-\mathbf{Q}_1}|^2 + |\Delta_{-\mathbf{Q}_1}|^2 |\Delta_{\mathbf{Q}_2}|^2 + |\Delta_{-\mathbf{Q}_2}|^2 |\Delta_{\mathbf{Q}_3}|^2 + |\Delta_{-\mathbf{Q}_3}|^2 |\Delta_{\mathbf{Q}_1}|^2 \right) \\
&+ g_\phi^{(4)} \left[(\Delta_{\mathbf{Q}_1}^2)(\Delta_{-\mathbf{Q}_1}^2)^* + (\Delta_{\mathbf{Q}_2}^2)(\Delta_{-\mathbf{Q}_2}^2)^* + (\Delta_{\mathbf{Q}_3}^2)(\Delta_{-\mathbf{Q}_3}^2)^* + c.c. \right] \\
&+ g_\theta^{(4)} \left[(\Delta_{\mathbf{Q}_1} \Delta_{-\mathbf{Q}_1})(\Delta_{\mathbf{Q}_2} \Delta_{-\mathbf{Q}_2})^* + (\Delta_{\mathbf{Q}_2} \Delta_{-\mathbf{Q}_2})(\Delta_{\mathbf{Q}_3} \Delta_{-\mathbf{Q}_3})^* + (\Delta_{\mathbf{Q}_3} \Delta_{-\mathbf{Q}_3})(\Delta_{\mathbf{Q}_1} \Delta_{-\mathbf{Q}_1})^* + c.c. \right],
\end{aligned} \tag{S15}$$

where $g_1^{(4)}$, $g_2^{(4)}$, $g_3^{(4)}$, $g_4^{(4)}$, $g_\phi^{(4)}$ and $g_\theta^{(4)}$ are the corresponding $\Delta_{\pm\mathbf{Q}_\alpha}$ -independent coefficients. For $\Delta_{\pm\mathbf{Q}_\alpha} = \Delta e^{i\theta_\alpha} e^{\pm i\frac{\phi_\alpha}{2}}$, we have

$$\mathcal{F}^{(4)} = 6 \left(g_1^{(4)} + \frac{g_2^{(4)}}{2} + g_3^{(4)} + g_4^{(4)} \right) \Delta^4 + 2g_\phi^{(4)} \Delta^4 \sum_{\alpha=1}^3 \cos(2\phi_\alpha) + 2g_\theta^{(4)} \Delta^4 [\cos(2\theta_2 - 2\theta_1) + \cos(2\theta_3 - 2\theta_2) + \cos(2\theta_1 - 2\theta_3)]. \tag{S16}$$

We are interested in the signs of $g_\phi^{(4)}$ and $g_\theta^{(4)}$ since they determine the values of ϕ_α and θ_α that minimize the free energy respectively. According to Eq. (S13) and Eqs. (S14), $g_\phi^{(4)}$ and $g_\theta^{(4)}$ can be expressed as

$$g_\phi^{(4)} = \frac{1}{2\beta} \sum_n \sum_{\mathbf{k}}' \frac{1}{(i\omega_n - \xi_{\mathbf{k}})(i\omega_n - \xi_{\mathbf{k}+2\mathbf{Q}_1})(i\omega_n + \xi_{-\mathbf{k}+\mathbf{Q}_1})(i\omega_n + \xi_{-\mathbf{k}-\mathbf{Q}_1})}, \tag{S17a}$$

$$g_\theta^{(4)} = \frac{1}{\beta} \sum_n \sum_{\mathbf{k}}' \frac{1}{(i\omega_n - \xi_{\mathbf{k}})(i\omega_n - \xi_{\mathbf{k}-\mathbf{Q}_1})(i\omega_n + \xi_{-\mathbf{k}-\mathbf{Q}_2})(i\omega_n + \xi_{-\mathbf{k}-\mathbf{Q}_3})} + \frac{1}{(i\omega_n - \xi_{\mathbf{k}})(i\omega_n - \xi_{\mathbf{k}+\mathbf{Q}_2-\mathbf{Q}_3})(i\omega_n + \xi_{-\mathbf{k}-\mathbf{Q}_2})(i\omega_n + \xi_{-\mathbf{k}+\mathbf{Q}_3})}, \tag{S17b}$$

where we have used $\xi_{\mathbf{k}} = \xi_{-\mathbf{k}}$ to combine terms in $g_\theta^{(4)}$. Now we can use the following formula to achieve the summation over $i\omega_n$,

$$\begin{aligned}
&\frac{1}{\beta} \sum_n \frac{1}{(i\omega_n - \xi_{\mathbf{k}_i})(i\omega_n - \xi_{\mathbf{k}_j})(i\omega_n + \xi_{\mathbf{k}_p})(i\omega_n + \xi_{\mathbf{k}_q})} \\
&= \frac{n_F(\xi_{\mathbf{k}_i})}{(\xi_{\mathbf{k}_i} - \xi_{\mathbf{k}_j})(\xi_{\mathbf{k}_i} + \xi_{\mathbf{k}_p})(\xi_{\mathbf{k}_i} + \xi_{\mathbf{k}_q})} + \frac{n_F(\xi_{\mathbf{k}_j})}{(\xi_{\mathbf{k}_j} - \xi_{\mathbf{k}_i})(\xi_{\mathbf{k}_j} + \xi_{\mathbf{k}_p})(\xi_{\mathbf{k}_j} + \xi_{\mathbf{k}_q})} \\
&+ \frac{n_F(-\xi_{\mathbf{k}_p})}{(\xi_{\mathbf{k}_i} + \xi_{\mathbf{k}_p})(\xi_{\mathbf{k}_j} + \xi_{\mathbf{k}_p})(\xi_{\mathbf{k}_q} - \xi_{\mathbf{k}_p})} + \frac{n_F(-\xi_{\mathbf{k}_q})}{(\xi_{\mathbf{k}_i} + \xi_{\mathbf{k}_q})(\xi_{\mathbf{k}_j} + \xi_{\mathbf{k}_q})(\xi_{\mathbf{k}_p} - \xi_{\mathbf{k}_q})},
\end{aligned} \tag{S18}$$

where n_F is the Fermi-Dirac distribution function.

By performing the summation over $i\omega_n$, $g_\phi^{(4)}$ is of the following form,

$$\begin{aligned} g_\phi^{(4)} &= \frac{1}{2} \sum_{\mathbf{k}}' \frac{n_F(\xi_{\mathbf{k}})}{(\xi_{\mathbf{k}} - \xi_{\mathbf{k}+2\mathbf{Q}_1})(\xi_{\mathbf{k}} + \xi_{-\mathbf{k}+\mathbf{Q}_1})(\xi_{\mathbf{k}} + \xi_{-\mathbf{k}-\mathbf{Q}_1})} + \frac{n_F(\xi_{\mathbf{k}+2\mathbf{Q}_1})}{(\xi_{\mathbf{k}+2\mathbf{Q}_1} - \xi_{\mathbf{k}})(\xi_{\mathbf{k}+2\mathbf{Q}_1} + \xi_{-\mathbf{k}+\mathbf{Q}_1})(\xi_{\mathbf{k}+2\mathbf{Q}_1} + \xi_{-\mathbf{k}-\mathbf{Q}_1})} \\ &\quad + \frac{n_F(-\xi_{-\mathbf{k}+\mathbf{Q}_1})}{(\xi_{\mathbf{k}} + \xi_{-\mathbf{k}+\mathbf{Q}_1})(\xi_{\mathbf{k}+2\mathbf{Q}_1} + \xi_{-\mathbf{k}+\mathbf{Q}_1})(\xi_{-\mathbf{k}-\mathbf{Q}_1} - \xi_{-\mathbf{k}+\mathbf{Q}_1})} + \frac{n_F(-\xi_{-\mathbf{k}-\mathbf{Q}_1})}{(\xi_{\mathbf{k}} + \xi_{-\mathbf{k}-\mathbf{Q}_1})(\xi_{\mathbf{k}+2\mathbf{Q}_1} + \xi_{-\mathbf{k}-\mathbf{Q}_1})(\xi_{-\mathbf{k}+\mathbf{Q}_1} - \xi_{-\mathbf{k}-\mathbf{Q}_1})} \\ &= \sum_{\mathbf{k}}' \frac{2n_F(\xi_{\mathbf{k}}) - 1}{(\xi_{\mathbf{k}} - \xi_{\mathbf{k}+2\mathbf{Q}_1})(\xi_{\mathbf{k}} + \xi_{-\mathbf{k}+\mathbf{Q}_1})(\xi_{\mathbf{k}} + \xi_{-\mathbf{k}-\mathbf{Q}_1})}, \end{aligned} \quad (\text{S19})$$

where we have used $n_F(x) + n_F(-x) = 1$. Due to the energy cutoff Λ , only the summation near the FS segment defined by $k_x = \pm\pi$ will give rise to a sizable contribution to the expression above. Notice that near $k_x = \pm\pi$, the following relation that represents the nesting feature of the hexagonal FS holds,

$$\xi_{\mathbf{k}+2\mathbf{Q}_1} \simeq -\xi_{\mathbf{k}}, \quad \xi_{-\mathbf{k}-\mathbf{Q}_1} \simeq -\xi_{-\mathbf{k}+\mathbf{Q}_1},$$

In the low-energy limit ($|\beta\xi_{\mathbf{k}}| \ll 1$), the function $2n_F(\xi_{\mathbf{k}}) - 1$ can be expanded as follows

$$2n_F(\xi_{\mathbf{k}}) - 1 \simeq -\frac{\beta\xi_{\mathbf{k}}}{2} + \frac{\beta^3\xi_{\mathbf{k}}^3}{24}.$$

Then we have

$$g_\phi^{(4)} \simeq \sum_{\mathbf{k}}' \frac{-\frac{\beta\xi_{\mathbf{k}}}{2} + \frac{\beta^3\xi_{\mathbf{k}}^3}{24}}{2\xi_{\mathbf{k}}(\xi_{\mathbf{k}}^2 - \xi_{-\mathbf{k}+\mathbf{Q}_1}^2)} = \sum_{\mathbf{k}}' -\frac{\beta}{4(\xi_{\mathbf{k}}^2 - \xi_{-\mathbf{k}+\mathbf{Q}_1}^2)} + \frac{\beta^3\xi_{\mathbf{k}}^2}{48(\xi_{\mathbf{k}}^2 - \xi_{-\mathbf{k}+\mathbf{Q}_1}^2)}.$$

By taking the substitution $\mathbf{k} \rightarrow -\mathbf{k} + \mathbf{Q}_1$ and adding it to the original expression, we obtain the following expression,

$$g_\phi^{(4)} \simeq \sum_{\mathbf{k}}' \frac{\beta^3(\xi_{\mathbf{k}}^2 - \xi_{-\mathbf{k}+\mathbf{Q}_1}^2)}{96(\xi_{\mathbf{k}}^2 - \xi_{-\mathbf{k}+\mathbf{Q}_1}^2)} = \sum_{\mathbf{k}}' \frac{\beta^3}{96} > 0. \quad (\text{S20})$$

We draw the conclusion that $g_\phi^{(4)}$ is positive.

We now focus on the derivation of $g_\theta^{(4)}$. Similarly, we perform the summation over $i\omega_n$ at first,

$$\begin{aligned} &\frac{1}{\beta} \sum_n \sum_{\mathbf{k}}' \frac{1}{(i\omega_n - \xi_{\mathbf{k}})(i\omega_n - \xi_{\mathbf{k}-\mathbf{Q}_1})(i\omega_n + \xi_{-\mathbf{k}-\mathbf{Q}_2})(i\omega_n + \xi_{-\mathbf{k}-\mathbf{Q}_3})} \\ &= \sum_{\mathbf{k}}' \frac{n_F(\xi_{\mathbf{k}})}{(\xi_{\mathbf{k}} - \xi_{\mathbf{k}-\mathbf{Q}_1})(\xi_{\mathbf{k}} + \xi_{-\mathbf{k}-\mathbf{Q}_2})(\xi_{\mathbf{k}} + \xi_{-\mathbf{k}-\mathbf{Q}_3})} + \frac{n_F(\xi_{\mathbf{k}-\mathbf{Q}_1})}{(\xi_{\mathbf{k}-\mathbf{Q}_1} - \xi_{\mathbf{k}})(\xi_{\mathbf{k}-\mathbf{Q}_1} + \xi_{-\mathbf{k}-\mathbf{Q}_2})(\xi_{\mathbf{k}-\mathbf{Q}_1} + \xi_{-\mathbf{k}-\mathbf{Q}_3})} \\ &\quad + \frac{n_F(-\xi_{-\mathbf{k}-\mathbf{Q}_2})}{(\xi_{\mathbf{k}} + \xi_{-\mathbf{k}-\mathbf{Q}_2})(\xi_{\mathbf{k}-\mathbf{Q}_1} + \xi_{-\mathbf{k}-\mathbf{Q}_2})(\xi_{-\mathbf{k}-\mathbf{Q}_3} - \xi_{-\mathbf{k}-\mathbf{Q}_2})} + \frac{n_F(-\xi_{-\mathbf{k}-\mathbf{Q}_3})}{(\xi_{\mathbf{k}} + \xi_{-\mathbf{k}-\mathbf{Q}_3})(\xi_{\mathbf{k}-\mathbf{Q}_1} + \xi_{-\mathbf{k}-\mathbf{Q}_3})(\xi_{-\mathbf{k}-\mathbf{Q}_2} - \xi_{-\mathbf{k}-\mathbf{Q}_3})} \\ &= 2 \sum_{\mathbf{k}}' \frac{n_F(\xi_{\mathbf{k}})}{(\xi_{\mathbf{k}} - \xi_{\mathbf{k}-\mathbf{Q}_1})(\xi_{\mathbf{k}} + \xi_{-\mathbf{k}-\mathbf{Q}_2})(\xi_{\mathbf{k}} + \xi_{-\mathbf{k}-\mathbf{Q}_3})} - \frac{n_F(-\xi_{\mathbf{k}})}{(\xi_{\mathbf{k}} - \xi_{\mathbf{k}+\mathbf{Q}_3-\mathbf{Q}_2})(\xi_{\mathbf{k}} + \xi_{-\mathbf{k}+\mathbf{Q}_2})(\xi_{\mathbf{k}} + \xi_{-\mathbf{k}-\mathbf{Q}_3})} \end{aligned} \quad (\text{S21a})$$

$$\begin{aligned} &\frac{1}{\beta} \sum_n \sum_{\mathbf{k}}' \frac{1}{(i\omega_n - \xi_{\mathbf{k}})(i\omega_n - \xi_{\mathbf{k}+\mathbf{Q}_2-\mathbf{Q}_3})(i\omega_n + \xi_{-\mathbf{k}-\mathbf{Q}_2})(i\omega_n + \xi_{-\mathbf{k}+\mathbf{Q}_3})} \\ &= \sum_{\mathbf{k}}' \frac{n_F(\xi_{\mathbf{k}})}{(\xi_{\mathbf{k}} - \xi_{\mathbf{k}+\mathbf{Q}_2-\mathbf{Q}_3})(\xi_{\mathbf{k}} + \xi_{-\mathbf{k}-\mathbf{Q}_2})(\xi_{\mathbf{k}} + \xi_{-\mathbf{k}+\mathbf{Q}_3})} + \frac{n_F(\xi_{\mathbf{k}+\mathbf{Q}_2-\mathbf{Q}_3})}{(\xi_{\mathbf{k}+\mathbf{Q}_2-\mathbf{Q}_3} - \xi_{\mathbf{k}})(\xi_{\mathbf{k}+\mathbf{Q}_2-\mathbf{Q}_3} + \xi_{-\mathbf{k}-\mathbf{Q}_2})(\xi_{\mathbf{k}+\mathbf{Q}_2-\mathbf{Q}_3} + \xi_{-\mathbf{k}+\mathbf{Q}_3})} \\ &\quad + \frac{n_F(-\xi_{-\mathbf{k}-\mathbf{Q}_2})}{(\xi_{\mathbf{k}} + \xi_{-\mathbf{k}-\mathbf{Q}_2})(\xi_{\mathbf{k}+\mathbf{Q}_2-\mathbf{Q}_3} + \xi_{-\mathbf{k}-\mathbf{Q}_2})(\xi_{-\mathbf{k}+\mathbf{Q}_3} - \xi_{-\mathbf{k}-\mathbf{Q}_2})} + \frac{n_F(-\xi_{-\mathbf{k}+\mathbf{Q}_3})}{(\xi_{\mathbf{k}} + \xi_{-\mathbf{k}+\mathbf{Q}_3})(\xi_{\mathbf{k}+\mathbf{Q}_2-\mathbf{Q}_3} + \xi_{-\mathbf{k}+\mathbf{Q}_3})(\xi_{-\mathbf{k}-\mathbf{Q}_2} - \xi_{-\mathbf{k}+\mathbf{Q}_3})} \\ &= 2 \sum_{\mathbf{k}}' \frac{n_F(\xi_{\mathbf{k}})}{(\xi_{\mathbf{k}} - \xi_{\mathbf{k}+\mathbf{Q}_2-\mathbf{Q}_3})(\xi_{\mathbf{k}} + \xi_{-\mathbf{k}-\mathbf{Q}_2})(\xi_{\mathbf{k}} + \xi_{-\mathbf{k}+\mathbf{Q}_3})} - \frac{n_F(-\xi_{\mathbf{k}})}{(\xi_{\mathbf{k}} - \xi_{\mathbf{k}+\mathbf{Q}_1})(\xi_{\mathbf{k}} + \xi_{-\mathbf{k}+\mathbf{Q}_2})(\xi_{\mathbf{k}} + \xi_{-\mathbf{k}+\mathbf{Q}_3})} \end{aligned} \quad (\text{S21b})$$

Then $g_\theta^{(4)}$ is of the following form,

$$g_\theta^{(4)} = g_{\theta,1}^{(4)} + g_{\theta,2}^{(4)}, \quad (\text{S22a})$$

$$g_{\theta,1}^{(4)} = 2 \sum_{\mathbf{k}}' \frac{2n_F(\xi_{\mathbf{k}}) - 1}{(\xi_{\mathbf{k}} - \xi_{\mathbf{k}+\mathbf{Q}_2-\mathbf{Q}_3})(\xi_{\mathbf{k}} + \xi_{-\mathbf{k}-\mathbf{Q}_2})(\xi_{\mathbf{k}} + \xi_{-\mathbf{k}+\mathbf{Q}_3})}, \quad (\text{S22b})$$

$$g_{\theta,2}^{(4)} = 2 \sum_{\mathbf{k}}' \frac{2n_F(\xi_{\mathbf{k}}) - 1}{(\xi_{\mathbf{k}} - \xi_{\mathbf{k}+\mathbf{Q}_1})(\xi_{\mathbf{k}} + \xi_{-\mathbf{k}+\mathbf{Q}_2})(\xi_{\mathbf{k}} + \xi_{-\mathbf{k}+\mathbf{Q}_3})}. \quad (\text{S22c})$$

For $g_{\theta,1}^{(4)}$, only \mathbf{k} near $(0, 2\pi/\sqrt{3})$ or $(-\pi, 0)$ gives a sizable contribution to the summation above due to the energy cutoff. For $\mathbf{k} = (0, 2\pi/\sqrt{3}) + \mathbf{q}$, we have

$$\xi_{\mathbf{k}} \simeq \frac{1}{2}(q_x^2 - 3q_y^2), \xi_{\mathbf{k}+\mathbf{Q}_2-\mathbf{Q}_3} \simeq 2q_x, \xi_{-\mathbf{k}-\mathbf{Q}_2} \simeq -q_x + \sqrt{3}q_y, \xi_{-\mathbf{k}+\mathbf{Q}_3} \simeq -q_x - \sqrt{3}q_y,$$

where \mathbf{q} is a small vector. Similarly, for $\mathbf{k} = (-\pi, 0) + \mathbf{q}$, we have

$$\xi_{\mathbf{k}} \simeq -2q_x, \xi_{\mathbf{k}+\mathbf{Q}_2-\mathbf{Q}_3} \simeq \frac{1}{2}(q_x^2 - 3q_y^2), \xi_{-\mathbf{k}-\mathbf{Q}_2} \simeq q_x + \sqrt{3}q_y, \xi_{-\mathbf{k}+\mathbf{Q}_3} \simeq q_x - \sqrt{3}q_y.$$

Thus we can obtain the following approximation of $g_{\theta,1}^{(4)}$,

$$\begin{aligned} g_{\theta,1}^{(4)} &\simeq \sum_{\mathbf{q}} \frac{2n_F\left(\frac{1}{2}(q_x^2 - 3q_y^2)\right) - 1}{-q_x(-q_x + \sqrt{3}q_y)(-q_x - \sqrt{3}q_y)} + \frac{-\beta(-2q_x) + \frac{\beta^3(-2q_x)^3}{12}}{-2q_x(-q_x + \sqrt{3}q_y)(-q_x - \sqrt{3}q_y)} \\ &= \sum_{\mathbf{q}} -\frac{\beta}{q_x^2 - 3q_y^2} + \frac{\beta^3 q_x^2}{3(q_x^2 - 3q_y^2)}, \end{aligned} \quad (\text{S23})$$

where the first term in the first line vanishes since it changes sign under $\mathbf{q} \rightarrow -\mathbf{q}$.

For $g_{\theta,2}^{(4)}$, only \mathbf{k} near $(\pm\pi/2, \sqrt{3}\pi/2)$ gives a sizable contribution to the summation above. For $\mathbf{k} = (\pi/2, \sqrt{3}\pi/2) + \mathbf{q}$, we have

$$\xi_{\mathbf{k}} \simeq q_x + \sqrt{3}q_y, \xi_{\mathbf{k}+\mathbf{Q}_1} \simeq q_x - \sqrt{3}q_y, \xi_{-\mathbf{k}+\mathbf{Q}_2} \simeq -2q_x, \xi_{-\mathbf{k}+\mathbf{Q}_3} \simeq \frac{1}{2}(q_x^2 - 3q_y^2).$$

For $\mathbf{k} = (-\pi/2, \sqrt{3}\pi/2) + \mathbf{q}$, we have

$$\xi_{\mathbf{k}} \simeq -q_x + \sqrt{3}q_y, \xi_{\mathbf{k}+\mathbf{Q}_1} \simeq -q_x - \sqrt{3}q_y, \xi_{-\mathbf{k}+\mathbf{Q}_2} \simeq \frac{1}{2}(q_x^2 - 3q_y^2), \xi_{-\mathbf{k}+\mathbf{Q}_3} \simeq 2q_x.$$

Thus we can obtain the following approximation of $g_{\theta,2}^{(4)}$,

$$\begin{aligned} g_{\theta,2}^{(4)} &\simeq \sum_{\mathbf{q}} \frac{-\beta(q_x + \sqrt{3}q_y) + \frac{\beta^3(q_x + \sqrt{3}q_y)^3}{12}}{2\sqrt{3}q_y(-q_x + \sqrt{3}q_y)(q_x + \sqrt{3}q_y)} + \frac{-\beta(-q_x + \sqrt{3}q_y) + \frac{\beta^3(-q_x + \sqrt{3}q_y)^3}{12}}{2\sqrt{3}q_y(-q_x + \sqrt{3}q_y)(q_x + \sqrt{3}q_y)} \\ &= \sum_{\mathbf{q}} \frac{\beta}{q_x^2 - 3q_y^2} - \frac{\beta^3(q_x^2 + q_y^2)}{4(q_x^2 - 3q_y^2)}. \end{aligned} \quad (\text{S24})$$

Finally, we obtain the following expression,

$$g_\theta^{(4)} = g_{\theta,1}^{(4)} + g_{\theta,2}^{(4)} \simeq \sum_{\mathbf{q}} \frac{\beta^3(q_x^2 - 3q_y^2)}{12(q_x^2 - 3q_y^2)} = \sum_{\mathbf{q}} \frac{\beta^3}{12} > 0. \quad (\text{S25})$$

Hence, we find that $g_\theta^{(4)}$ is also positive.

For positive $g_\phi^{(4)}$ and $g_\theta^{(4)}$, according to Eq. (S16), we should minimize the following functions to obtain the minimum free energy up to Δ^4 ,

$$h_\phi = \cos(2\phi_1) + \cos(2\phi_2) + \cos(2\phi_3), \quad (\text{S26a})$$

$$h_\theta = \cos(2\theta_2 - 2\theta_1) + \cos(2\theta_3 - 2\theta_2) + \cos(2\theta_1 - 2\theta_3). \quad (\text{S26b})$$

It is easy to see that h_θ reaches its minimum -1 at $\phi_\alpha = \pm\pi/2$. For h_θ , let $x = \theta_2 - \theta_1$ and $y = \theta_3 - \theta_2$, we have

$$h_\theta = \cos(2x) + \cos(2y) + \cos(2(x+y)).$$

h_θ reaches its minimum $-3/2$ at $x = y = \pm 2\pi/3 \pmod{\pi}$. Thus, our PDW state acquires minimum free energy at $\phi = \pm\pi/2$ and $\theta_2 - \theta_1 = \theta_3 - \theta_2 = \pm 2\pi/3 \pmod{\pi}$, leading to a spatial inversion symmetry and TRS breaking state.

VI. LOCAL DENSITY OF STATES

Since there is no spin-flip effect, the charge density of the system is of the following form,

$$\rho(\mathbf{r}_i) = \frac{1}{N} \left(\langle c_{\mathbf{r}_i, \uparrow}^\dagger c_{\mathbf{r}_i, \uparrow} \rangle + \langle c_{\mathbf{r}_i, \downarrow}^\dagger c_{\mathbf{r}_i, \downarrow} \rangle \right) = \frac{2}{N} \langle c_{\mathbf{r}_i, \uparrow}^\dagger c_{\mathbf{r}_i, \uparrow} \rangle. \quad (\text{S27})$$

where $c_{\mathbf{r}_i, \uparrow(\downarrow)}^\dagger$ is fermion creation operator at site \mathbf{r}_i with spin $\uparrow(\downarrow)$. $\langle \rangle$ denotes the expectation value. By performing the Fourier transformation $c_{\mathbf{r}_i, \sigma} = \frac{1}{\sqrt{N}} \sum_{\mathbf{k}} e^{i\mathbf{k} \cdot \mathbf{r}_i} c_{\mathbf{k}, \sigma}$, we obtain the charge density in \mathbf{q} space,

$$\rho(\mathbf{q}) = \sum_{\mathbf{r}_i} e^{-i\mathbf{q} \cdot \mathbf{r}_i} \rho(\mathbf{r}_i) = \frac{2}{N} \sum_{\mathbf{r}_i} e^{-i\mathbf{q} \cdot \mathbf{r}_i} \langle c_{\mathbf{r}_i, \uparrow}^\dagger c_{\mathbf{r}_i, \uparrow} \rangle = \frac{2}{N^2} \sum_{\mathbf{r}_i} \sum_{\mathbf{k}, \mathbf{k}'} e^{-i(\mathbf{k}-\mathbf{k}'+\mathbf{q}) \cdot \mathbf{r}_i} \langle c_{\mathbf{k}, \uparrow}^\dagger c_{\mathbf{k}', \uparrow} \rangle = \frac{2}{N} \sum_{\mathbf{k}} \langle c_{\mathbf{k}, \uparrow}^\dagger c_{\mathbf{k}+\mathbf{q}, \uparrow} \rangle. \quad (\text{S28})$$

Using Eqs. (5) in the main text, $\rho(\mathbf{q})$ can be expressed in terms of Bogoliubov quasi-particle $\gamma_{\mathbf{k}, \sigma, i}$,

$$\begin{aligned} \rho(\mathbf{q}) &= \frac{2}{N} \sum_{\mathbf{k}} \sum_{j,l} \left(\langle u_{1j}(\mathbf{k}) \gamma_{\mathbf{k}, \uparrow, j}^\dagger + v_{1j}(\mathbf{k}) \gamma_{-\mathbf{k}, \downarrow, j} \rangle (u_{1l}^*(\mathbf{k}+\mathbf{q}) \gamma_{\mathbf{k}+\mathbf{q}, \uparrow, l} + v_{1l}^*(\mathbf{k}+\mathbf{q}) \gamma_{-\mathbf{k}-\mathbf{q}, \downarrow, l}^\dagger) \right) \\ &= \frac{2}{N} \sum_{\mathbf{k}} \sum_{j,l} u_{1j}(\mathbf{k}) u_{1l}^*(\mathbf{k}+\mathbf{q}) \langle \gamma_{\mathbf{k}, \uparrow, j}^\dagger \gamma_{\mathbf{k}+\mathbf{q}, \uparrow, l} \rangle + v_{1j}(\mathbf{k}) v_{1l}^*(\mathbf{k}+\mathbf{q}) \langle \gamma_{-\mathbf{k}, \downarrow, j} \gamma_{-\mathbf{k}-\mathbf{q}, \downarrow, l}^\dagger \rangle \\ &= \frac{2}{N} \sum_{\mathbf{k}} \sum_j \left[u_{1j}(\mathbf{k}) u_{1j}^*(\mathbf{k}+\mathbf{q}) \langle \gamma_{\mathbf{k}, \uparrow, j}^\dagger \gamma_{\mathbf{k}, \uparrow, j} \rangle + v_{1j}(\mathbf{k}) v_{1j}^*(\mathbf{k}+\mathbf{q}) \langle \gamma_{-\mathbf{k}, \downarrow, j} \gamma_{-\mathbf{k}, \downarrow, j}^\dagger \rangle \right] \bar{\delta}_{\mathbf{k}, \mathbf{k}+\mathbf{q}} \\ &= \frac{2}{N} \sum_{\mathbf{k}} \sum_j \left[u_{1j}(\mathbf{k}) u_{1j}^*(\mathbf{k}+\mathbf{q}) n_F(E(\mathbf{k})_j^+) + v_{1j}(\mathbf{k}) v_{1j}^*(\mathbf{k}+\mathbf{q}) n_F(E(\mathbf{k})_j^-) \right] \bar{\delta}_{\mathbf{k}, \mathbf{k}+\mathbf{q}}, \end{aligned} \quad (\text{S29})$$

where we use $\langle \gamma_{\mathbf{k}, \uparrow, j}^\dagger \gamma_{\mathbf{k}', \uparrow, l} \rangle = n_F(E(\mathbf{k})_j^+) \bar{\delta}_{\mathbf{k}, \mathbf{k}'} \delta_{j,l}$ and $\langle \gamma_{-\mathbf{k}, \downarrow, j} \gamma_{-\mathbf{k}', \downarrow, l}^\dagger \rangle = n_F(E(\mathbf{k})_j^-) \bar{\delta}_{\mathbf{k}, \mathbf{k}'} \delta_{j,l}$. Here

$$\bar{\delta}_{\mathbf{k}, \mathbf{k}'} = \begin{cases} 1, & \mathbf{k} - \mathbf{k}' = m\mathbf{Q}_1 + n\mathbf{Q}_2, m, n \in \mathcal{Z} \\ 0, & \text{otherwise} \end{cases}$$

Thus, the Fourier transformation of the LDOS, $\rho(\mathbf{q}, \omega)$ reads

$$\rho(\mathbf{q}, \omega) = -\frac{2}{N} \sum_{\mathbf{k}} \sum_j \left[u(\mathbf{k})_{1j} u^*(\mathbf{k}+\mathbf{q})_{1j} \frac{\partial n_F(\omega - E(\mathbf{k})_j^+)}{\partial \omega} + v(\mathbf{k})_{1j} v^*(\mathbf{k}+\mathbf{q})_{1j} \frac{\partial n_F(\omega - E(\mathbf{k})_j^-)}{\partial \omega} \right] \bar{\delta}_{\mathbf{k}, \mathbf{k}+\mathbf{q}}. \quad (\text{S30})$$

Using the folding property, Eq. (S30) can be written into the following form,

$$\rho(\mathbf{q}, \omega) = -\frac{1}{8N} \sum_{\mathbf{k}} \sum_{i,j=1}^{16} \left[u(\mathbf{k})_{ij} u^*(\mathbf{k}+\mathbf{q})_{ij} \frac{\partial n_F(\omega - E(\mathbf{k})_j^+)}{\partial \omega} + v(\mathbf{k})_{ij} v^*(\mathbf{k}+\mathbf{q})_{ij} \frac{\partial n_F(\omega - E(\mathbf{k})_j^-)}{\partial \omega} \right] \bar{\delta}_{\mathbf{k}, \mathbf{k}+\mathbf{q}}. \quad (\text{S31})$$

We can see from Eq. (S31) that $\mathbf{q} = m\mathbf{Q}_1 + n\mathbf{Q}_2$ ($m, n \in \mathcal{Z}$) is necessary for $\rho(\mathbf{q}, \omega)$ being nonzero. Taking into account the symmetry of the system and $\rho(\mathbf{q}, \omega) = \rho^*(-\mathbf{q}, \omega)$, there are four possible nonzero $|\rho(\mathbf{q}, \omega)|$ in the BZ,

$$\rho_A(\omega) = |\rho(\mathbf{q} = \mathbf{0}, \omega)|, \quad (\text{S32a})$$

$$\rho_B(\omega) = |\rho(\mathbf{q} = \pm\mathbf{Q}_1, \omega)| = |\rho(\mathbf{q} = \pm\mathbf{Q}_2, \omega)| = |\rho(\mathbf{q} = \pm\mathbf{Q}_3, \omega)|, \quad (\text{S32b})$$

$$\rho_C(\omega) = |\rho(\mathbf{q} = \pm 2\mathbf{Q}_1, \omega)| = |\rho(\mathbf{q} = \pm 2\mathbf{Q}_2, \omega)| = |\rho(\mathbf{q} = \pm 2\mathbf{Q}_3, \omega)|, \quad (\text{S32c})$$

$$\rho_D(\omega) = |\rho(\mathbf{q} = \pm(\mathbf{Q}_1 - \mathbf{Q}_2), \omega)| = |\rho(\mathbf{q} = \pm(\mathbf{Q}_2 - \mathbf{Q}_3), \omega)| = |\rho(\mathbf{q} = \pm(\mathbf{Q}_3 - \mathbf{Q}_1), \omega)|. \quad (\text{S32d})$$

$\rho_A(\omega)$ is just the DOS $\rho(\omega)$ we calculated in the main text.